Comparative Morphometrics of the Sacral Vertebra

in *Aneides* (Caudata: Plethodontidae)

_____

A thesis

presented to

the faculty of the Department of Biology

East Tennessee State University

In partial fulfillment

of the requirements for the degree

Master of Science in Biology

_____

by

Lisa Schaaf

May 2010

_____

Dr. Jim I. Mead, Chair

Dr. Blaine W. Schubert

Dr. Steven C. Wallace

Keywords: *Aneides,* Plethodontidae, comparative osteology, geometric morphometrics

ABSTRACT

Comparative Morphometrics of the Sacral Vertebra

in *Aneides* (Caudata: Plethodontidae)

by

Lisa Schaaf

The genus *Aneides* (Caudata: Plethodontidae) is an arboreal salamander with a prehensile tail and a distribution that spans North America. It is hypothesized that adaptations for arboreality will be visible in the osteology of the sacral vertebra either by qualitative analysis or linear and morphometric analysis in comparison with other plethodontid salamanders. This study demonstrates that while qualitative and quantitative analyses are successful at making genus-level distinctions between taxa, identification to lower taxonomic levels remains inconclusive. Linear morphometrics and dorsal Procrustes landmarks were the most successful metrics to identify known taxa. Two unidentified fossil salamander sacral vertebrae from Oregon Caves National Monument are examined with the same techniques and are tentatively identified as *Hydromantes* based on qualitative similarities to modern *Hydromantes* specimens, as the quantitative analyses were unable to confidently diagnose the unkonwn specimens.

ACKNOWLEDGEMENTS

CONTENTS

LIST OF FIGURES

CHAPTER 1

INTRODUCTION

The amphibian genus *Aneides*, a lungless salamander within the Plethodontidae, is found today

in the coastal regions of western North America, an isolated mountain range in southern New Mexico,

and the greater Appalachian region of the east. Among plethodontid salamanders, the clade *Aneides* is

one of the more derived genera and is known for its climbing specializations including a prehensile tail

(Petranka 1998). It is a small clade that includes 6 species: *A. aeneus, A. ferreus, A. vagrans, A.*

flavipunctatus, A. hardii, and *A. lugubris*. Wake and Jackman (1998) and Jackman (1998) differentiate

A. ferreus and *A. vagrans* based on a number of genetic differences but note that, in their view, the

species are osteologically identical.

Here I provide a morphometric study of the sacral vertebra of *Aneides*. For the purposes of this

study, *A. ferreus* and *A. vagrans* have been treated as one taxon and will be referred to as *A. ferreus*.

Also included in this study are other species of salamanders including Rhyacotritionidae

(*Rhyacotrition*) and Plethodontidae (*Plethodon elongatus, Plethodon dunni, Hydromantes shastae,*

Ensatina eschscholtzii). Fossil salamanders have been included to increase the size, robustness, and

diversity of the dataset, to provide context for morphological differentiation between species, and to

help identify fossil salamanders from Oregon Caves National Monument (ORCA). Ideally, any analysis

of the osteological variation in *Aneides* as compared to other salamanders of the Plethodontidae should

reveal some insight into the unique adaptations for an arboreal lifestyle.

This study has two goals: First, to assess whether or not morphological variation can be seen in

the sacral vertebrae of salamanders and to compare and contrast the ability of traditional and geometric

morphometric techniques to define that variation. Second, this study will test these assumptions by

using analytical data to diagnose fossil salamander sacral vertebra from Oregon Caves National

Monument (ORCA). The importance of this project lies in its potential to address biogeographical questions concerning the historical distribution of plethodontid salamanders across North America. Although most data indicate stability in salamander faunas through time (Holman 2006), we can only guess at their historical distribution. The fossil record for salamanders is sparse at best, and this work represents a first step towards expanding that knowledge and a potential new approach to fossil identification.

<div align="center">Background</div>

Phylogeny

The Order Caudata (sometimes referred to as Urodela) is well-recognized as a monophyletic clade (Lannoo 2005, Holman 2006), but the relationships among the various salamander families are not clear (Larson and Dimmick 1993, Larson et al. 2003). Plethodontid salamanders in particular are not recognized as having close relatives among other extant salamanders (Larson et al. 2006). Phylogenies of plethodontid salamanders have traditionally been constructed on the basis of morphological variation (Wake 1963, Wake 1966), but molecular phylogenies (Larson and Dimmick 1993, Mueller 2004, Plotner et al. 2007) and combinations of molecular and morphological characteristics (Chippendale et al. 2004) have been used more recently.

Wake (1966) established some of the more detailed relationships within Plethodontidae. He divided the Plethodontidae into two subfamilies, the Plethodontinae and the Desmognathinae, and further subdivided Plethodontinae into three tribes, the Plethodontini, Hemidactyliini, and Bolitoglossini. He assigned *Plethodon, Aneides,* and *Ensatina* to the tribe Plethodontini and within that tribe concluded that *Plethodon* is the most basal of those taxa, while *Aneides* is the most derived (Wake 1966, Larson et al. 2006). Lombard and Wake (1986) revised this phylogeny in their study of the evolution of tongue-feeding in plethodontid salamanders. Based on morphological characters, they

concluded that although tongue-feeding is likely a characteristic of convergent evolution within the family as a whole, *Plethodon* and *Aneides* form a sister group, and *Ensatina* is the immediate outgroup. Larson and Dimmick (1993) proposed a monophyletic grouping for extant salamanders based on internal fertilization and supported by cloacal anatomical characters, but this phylogeny is not supported by molecular data either alone or in connection with morphological data and fossil taxa (Gao and Shubin, 2001; Larson et al. 2003).

Recent molecular studies have called the monophyly of the traditional subgroupings into question. Chippendale et al. (2004) (Figure 1), using a combined molecular and morphological approach to their study of life-history evolution in plethodontid salamanders, concluded that contrary to previous work, *Aneides* and *Ensatina* form a sister clade to the exclusion of *Plethodon*, which was considered basal to (Desmognathinae + (*Aneides* + *Ensatina*)). To further confound the issue, Mueller et al. (2004) (Figure 2) published a strictly molecular phylogeny of Plethodontidae that rejected monophyly of Plethodontini with respect to the desmognathine salamanders and *Hydromantes*. According to their study, *Aneides* forms a sister group with *Hydromantes, Ensatina* forms a sister group with *Desmognathus*, and *Plethodon* is basal to both clades. Plotner et al. (2007) summarized the competing phylogenetic hypotheses by noting that at the generic level, molecular systematic classification correlated with the morphological classification, but at the familial level the 2 methodologies conflicted. Plethodontid systematics continues to be problematic.
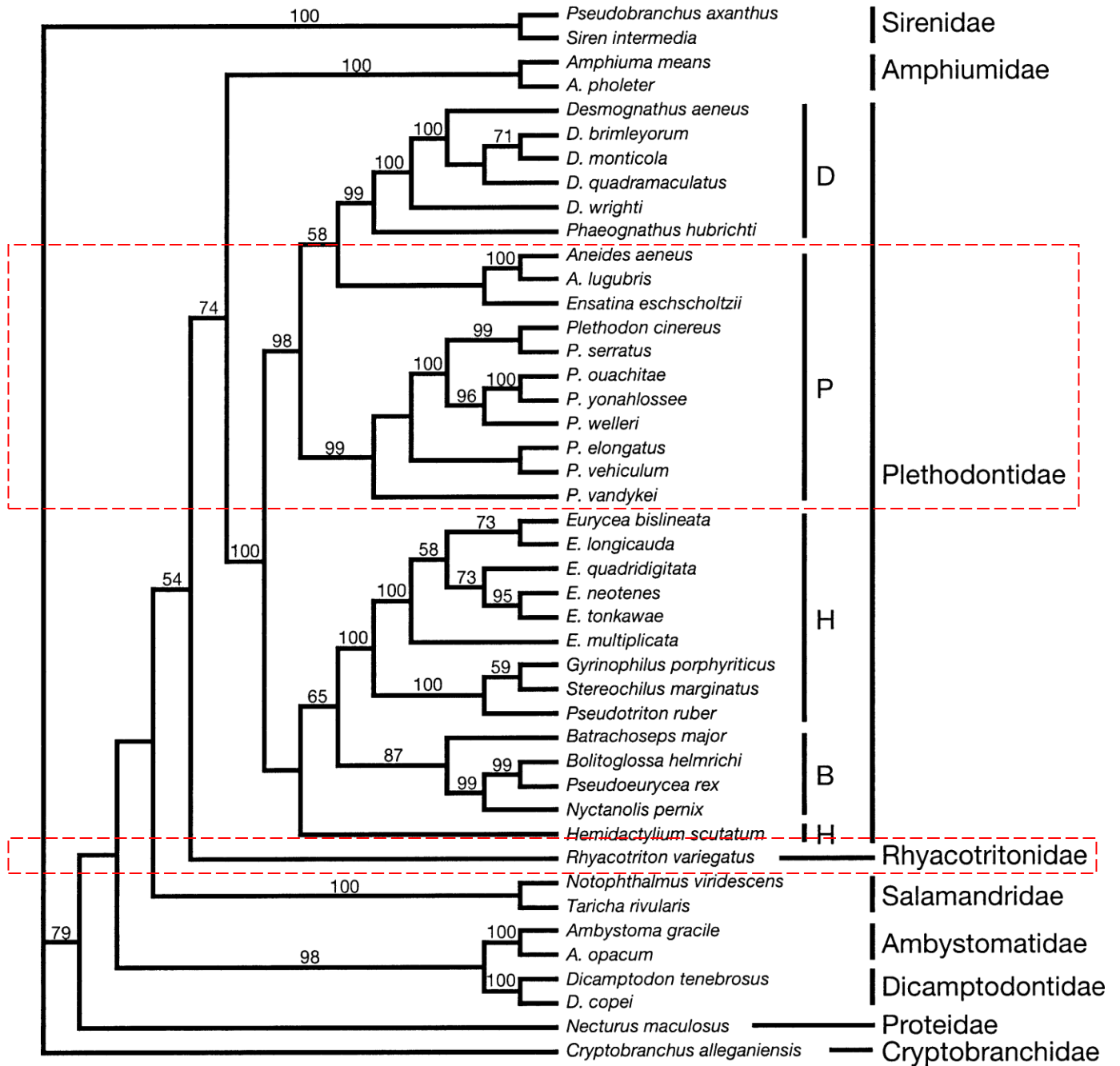
Figure 1: Salamander phylogeny (modified from Chippendale et al., 2004)
One of many phylogenies of salamander relationships. This phylogeny is based on a combination of mitochondrial and nuclear DNA and morphology. Highlighted sections indicate taxa included in this study. Modified from Chippendale et al. 2004.
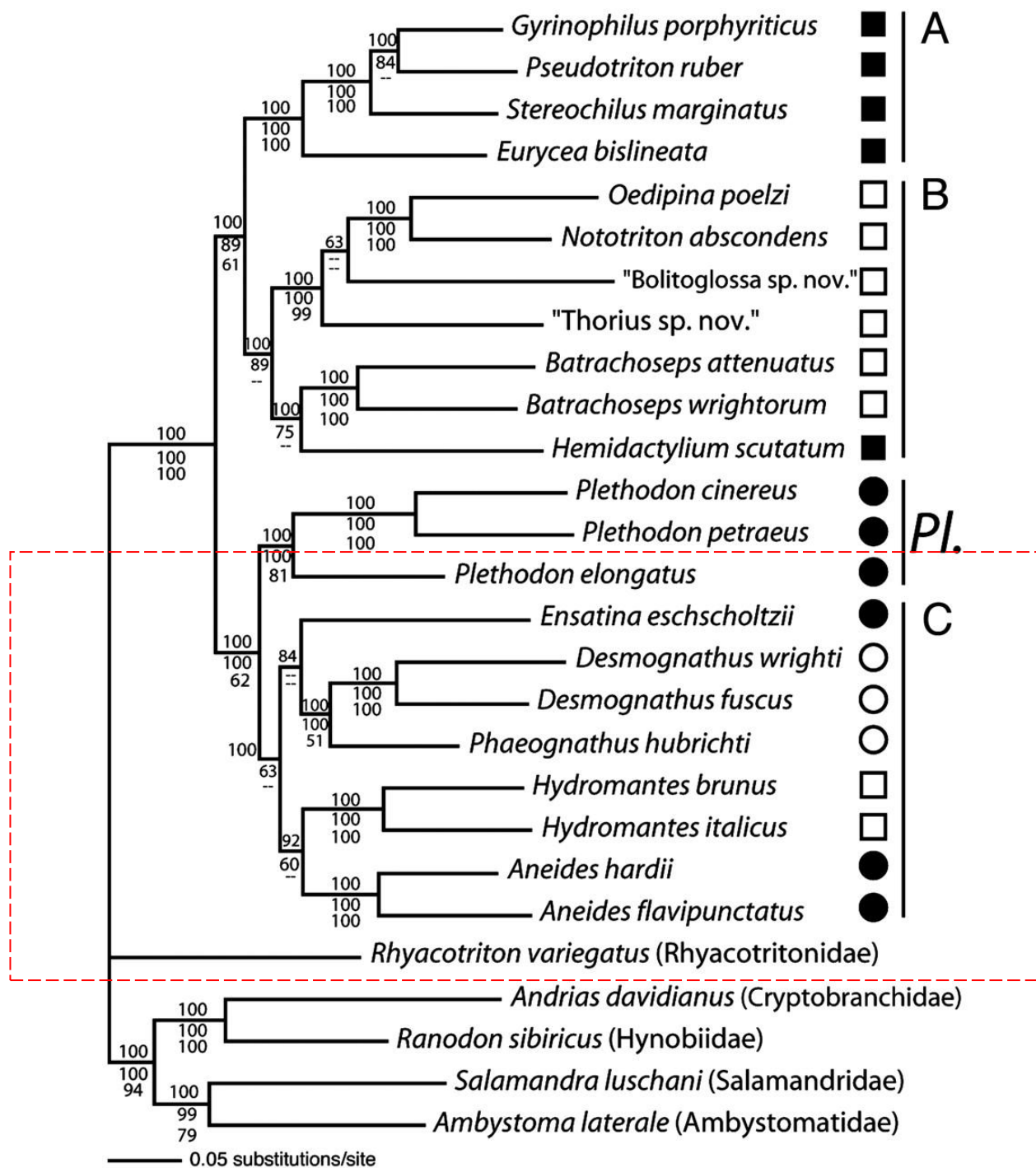
Figure 2: Salamander phylogeny (modified from Mueller et al., 2004)
One of the many accepted phylogenies of Caudata. Highlighted section indicates taxa included in this study. Modified from Mueller et al. 2004.

Distribution

As a member of the family Plethodontidae, *Aneides* species are lungless and thus require some moisture in their habitats. The greatest diversity in salamander species can be found in humid habitats such as the coastal rainforests of the American Northwest and the Appalachian Highlands of the southeast (Duellman and Sweet, 1999). *Aneides* is distributed across North America in a disjunct pattern (Figure 3). *A. aeneus* can be found in the southern Appalachians, *A. hardii* can be found as a small population in New Mexico, and *A. ferreus, A. lugubris,* and *A. flavipunctatus* inhabit humid, forested coastline from southern California to Vancouver Island in British Columbia, Canada.
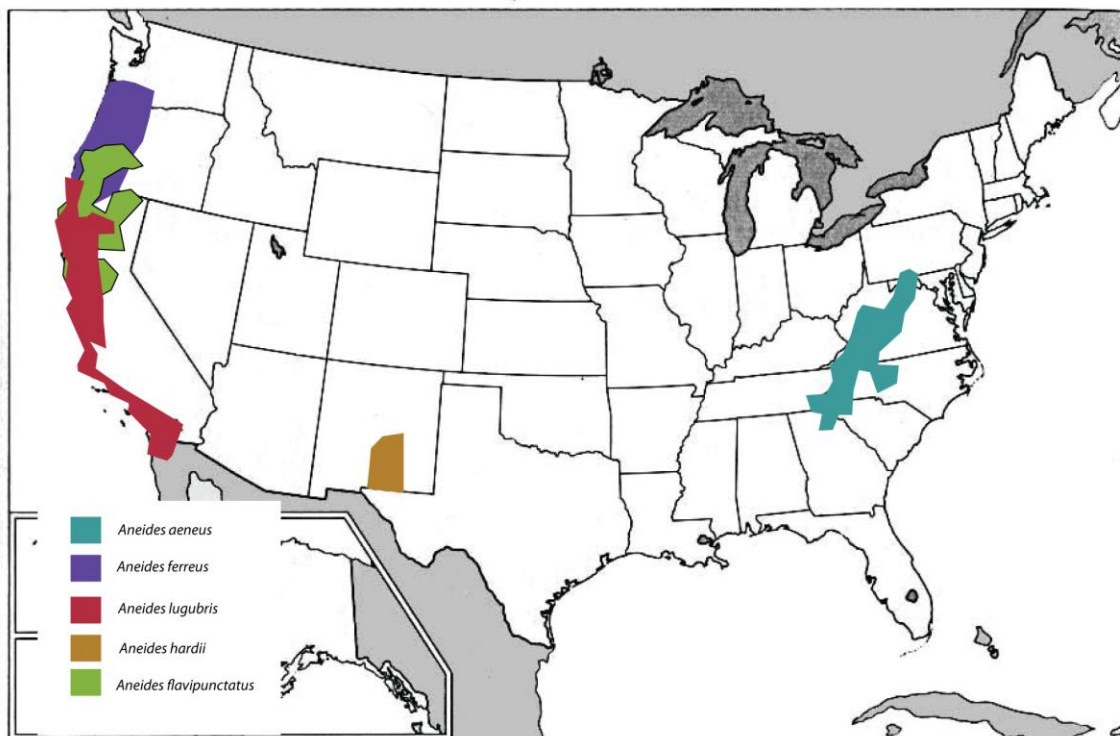
Figure 3: Map of current *Aneides* distribution . Modern distribution of all *Aneides* species included in this analysis. All data from the USGS National Amphibian Atlas.

The historical distribution of *Aneides* and of the tribe Plethodontini correlates with the distribution of the Arcto-Tertiary geoflora, which refers to a uniform broad-leaved deciduous forest stretching around the northern hemisphere in the temperate latitudes (Lowe 1950b, Wake 1966, Graham 1999). Graham (1999) notes this term is an oversimplification, as this floral assemblage included a prominent gymnosperm component (specifically, *Sequoia*), and its response to climate change was monolithic and uniform. The first disruption in the contiguity of this belt occurred in the midcontinent of North America, when the Cretaceous sea retreated and temperatures dropped, and tropical to warm deciduous flora were replaced by increasingly drier and more grass-dominated flora. This trend towards grasslands in the Plains and, with the uplift of the Rockies, montane coniferous forests in the west and deserts in the southwest, effectively eliminating the deciduous forests except for glacial refugia in the Appalachian region (Duellman and Sweet 1999, Graham 1999).

Plethodontine salamanders are assumed to be members of biotic communities dominated by floral derivatives of the Arcto-Tertiary geoflora (Lowe 1950b, Wake 1966). *Aneides* and *Plethodon* have disjunct eastern and western populations, respectively, of a once-continuous distribution, with the ancestral stock having its roots presumably somewhere in Appalachia and expansion occurring westward (Duellman and Sweet 1999). Apparently, disjunction began during the Miocene and was complete by the Pliocene. Two species, *Aneides hardii* and *Plethodon neomexicanus,* are usually held as examples of this disjunction; both are isolated populations above 2000m elevation in the Rocky Mountains, are well-defined species, and were probably able to adapt to favorable microhabitats as the climate and forest changed (Lowe 1950a, Wake 1966).

During the Quaternary period, glacial-interglacial cycles dominated the climate regime and shaped the topography of North America, while herpetofaunas from this period remained stable (Estes and Baez 1985, Holman 1995, Duellman and Sweet 1999). Fossil evidence of this historical

13

distribution is rare, at best, and subject to the vagaries of preservation. Holman (2006) notes that there are as many fossil salamanders from the Pleistocene Epoch of North America as there are in the other geologic epochs put together. The few *Aneides* fossils recorded are from the late Oligocene to early Miocene of Wyoming and the late Pleistocene of California (Holman, 2006). The most frequently preserved skeletal elements are vertebrae, and identification to species level based on these elements is difficult at best. Conclusive identification is often only possible at the generic level (Wake 1966, Holman 2006). Well-defined vertebral characters might enable more species-level identification of *Aneides* fossils. The study is designed to identify these characters and improve the potential for fossil salamander identification.

Osteology

Little work has been produced on the osteology of *Aneides*. Dunn (1926) created a diagnosis for the genus that included several unique cranial and some postcranial soft-tissue characteristics, but he did not address the postcranial osteology in detail. Hilton (1945) in his short paper of the cranial, axial, and appendicular skeleton of *Aneides* was the first to provide illustrations of the entire body. He also provided a list of "special features" of the skull but did not suggest if these were apomorphies. Lowe (1950b) in his discussion on systematics and biogeography of *Aneides* simplified Hilton's list of features into 3 diagnostic characters for the genus: 1) fusion of the premaxillae, 2) maxilla with posterior portion knife-edged and edentulous, and 3) terminal phalanges Y-shaped. Wake (1963) was the first to examine the skeleton of *Aneides* in depth. His 1963 paper on the osteology of the genus and a comparison to *Plethodon* and *Ensatina* used both cleared-and-stained and skeletonized specimens to identify diagnostic features for each element of the *Aneides* skeleton. In 1966 Wake published a paper outlining the comparative osteology and evolution of all the members of Plethodontidae, the goal of

which was to understand the functional and adaptive significance of osteological variation within the family. While Wake (1966) included taxa from almost all the other major salamander families, the study here focuses mostly on specific plethodontids by examining *Ensatina eschscholtzii* (4 specimens, Plethodontini), *Plethodon dunni* (2 specimens, Plethodontini), *P. elongatus* (3 specimens, Plethodontini), and *P. neomexicanus* (3 specimens, Plethodontini). These species are most closely related to *Aneides*, in the tribe Plethodontini. *Ensatina* has one species, thus the choice for that genus was obvious, but *Plethodon* is one of the most speciose genera in all of Caudata. *Plethodon dunni* and *P. elongatus* were chosen to represent some of the largest and smallest *Plethodon* species that occur in the same general area as the *Aneides* species under consideration. *Plethodon neomexicanus* was included because it was at one time considered to be conspecific with *Aneides hardii*. These 2 species share the same relict mountain habitat in New Mexico, and may have very similar sacral vertebrae. For the purposes of variation and to answer questions about the potential identification of the ORCA fossils, *Hydromantes shastae* (2 specimens, Bolitoglossini) and *Rhyacotrition variegatus* (2 specimens, Rhyacotritonidae) have been included. The inclusion of taxa from tribe, subfamily, and family levels will increase the overall robustness of the dataset by increasing morphological variation, and provide a point of reference for further morphological studies.

Given that *Aneides* is known for its unique locomotor adaptations for climbing, that it has a disjunct distribution across North America, and that there is variation in its current habitats, it is hypothesizes that one or another of these factors may have had an influence on the shape of the sacral vertebra. The choice of sacral vertebrae as the skeletal element to be studied was made for 2 reasons: this vertebra has not been studied in depth, and its placement within the vertebral column suggests the potential for information about locomotor morphospace. The sacral vertebra is, as Wake (1963) defines it, a well-developed trunk vertebra that stands at the transition between thoracic and caudal vertebrae,

and bears modified ribs for articulation with and support for the pelvic girdle. This definition is very helpful when looking at an articulated specimen. For disarticulated specimens where the transition between the thoracic and caudal vertebrae has been lost, the quickest way to differentiate between thoracic and caudal vertebrae is to look for distinctly separate transverse processes. It seems that the parapophysis and diapophysis are always separated on trunk vertebrae but are often fused or connected by a thin bone webbing on caudal vertebrae. Another distinguishing characteristic of a caudal vertebra is the presence of a ventral or haemal arch, but this is sometimes absent from the anteriormost caudal vertebra. To find the sacral vertebra, then, it is helpful to look for a trunk vertebra that is significantly wider and more robust than the other trunk vertebrae, with transverse processes that are much thicker and longer and often with cup-shaped tips. In fossil vertebrae where the tips of the transverse processes may have been worn away by postdepositional processes, a sacral vertebra can be determined based on the ratio between the length of the neural arch to the width of the neural arch at the posterior articulation of the transverse processes to the trunk, as sacral vertebrae in salamanders seem to be shorter and more stout than trunk vertebra.

CHAPTER 2

METHODS

Techniques

I chose to combine the 2 techniques of linear and geometric morphometrics to address my major

questions. The first goal is to assess potential differences or similarities of the various species of

Aneides, and the second goal is to address questions of paleoenvironmental interpretation and fossil

identification from ORCA. Here, a linear morphometrics (LM) approach is used in conjunction with a

geometric morphometrics (GM) approach. Linear measurements, as the traditional tool of choice for

morphologists, have become, in part, supplanted in recent years by the advent of geometric

morphometrics (Adams 2004) as a better overall approach to shape analysis (Maderbacher et al. 2008).

Both approaches seek to define homology of one organism relative to another, as a matter of

comparison of the same parts of the body in order to understand their function (Zelditch et al. 2004).

LM variables are generally linear measurements but can include ratios of linear measurements. They

represent the "extent" (Bookstein 1997) of physical distances or size as a description of part-to-part

homology, but homology can be obscured by size variation within the population. GM variables are

essentially the endpoints of linear measurements and should be considered as a "mapping function"

(Bookstein 1997) of point-to-point homology or shape without size. These endpoints are known as

landmarks and are defined as "discrete points that correspond among all the forms of a data set"

(Bookstein 1997). In theory the same information gained from LM variables can be gained from GM

landmarks, but the assumption of equivalence remains controversial (see Christiansen 2008 vs.

Maderbacher et al. 2008). There are 3 types of landmarks; Type 1 is the most easily replicable (for

example, at the junction of two sutures), Type 2 less so, and Type 3 is the least replicable. This analysis

17

uses a Procrustes fit as opposed to traditional Bookstein coordinates. This is a method of superimposition for landmark alignment that removes size, rotation, and scaling from the dataset to achieve the best alignment. This method has also been chosen as it permits the creation of thin-plate splines used as a visual aid to understanding location, intensity, and direction of shape change within the *Aneides* sacrum. Thin-plate splines can be thought of as a sheet of metal that bends and deforms according to the changes between landmarks, allowing the researcher to interpret what is happening between each landmark. Mathematically it is a smooth, continuous function that maps changes from one form to another (Zelditch et al. 2004).

In addition to TM and GM analysis techniques, I assess the validity of each set of results with a discriminant analysis (DA). Bookstein (1997), Zelditch et al. (2004), and Hammer and Harper (2006) provide excellent overviews of this technique. The DA is a statistical tool for separating cases into groups based on predictors. It produces a series of discriminant functions that most parsimoniously maximize the differences between groups, with the first function being the most important and each subsequent function controlling for the previous functions. All functions are associated with an eigenvalue that indicates the relative importance of each function to the overall separation, and with a canonical correlation that indicates correlation between the functions and each group. The DA also performs a test called Wilks' lambda to measure how each variable contributes to the function on a scale from 0-1. Also performed at the same time, the F-value of Wilks' lambda indicates the significance of each contribution. A large lambda value indicates great significance, but a smaller lambda value indicates low significance. The DA assumes that the sample size is adequate and errors are randomly distributed, that all cases are independent and continuous (interval), that the group sizes are not lopsided, that the groups are indeed a dichotomy, and that variance is similar between groups.

To test these assumptions, I use canonical plots where the 2 axes are the 2 most important

disciminant functions, and I identify the centroids of each grouping to depict what is referred to as a morphospace - the area on the plot occupied by one group as determined by the combination of 2 discriminant functions. To interpret these results, I use the structure coefficients to assess the set of variables that most heavily inform a given function to assign a meaningful label to that function.

Photographs were taken with a Leica Z16 APO microscope at 10 different computer-defined focal depths then montaged into a single, uniformly-focused image using the AutoMontage software suite. Landmarks and measurements were taken with the tpsDig suite of software (Rohlf, 2000).

<div align="center">

Measurements

</div>

Specimens used in this analysis are listed in Table 1. All measurements are listed in Table 2. All landmarks are listed in Table 3.

Table 1: Specimens used in analysis

Specimen	Genus/species		State/ county	
UCMVZ 189234	*Aneides*	*Aeneus*	AL	De Kalb
UCMVZ 189235	*Aneides*	*Aeneus*	AL	De Kalb
UCMVZ 189237	*Aneides*	*Aeneus*	AL	De Kalb
UCMVZ 189238	*Aneides*	*Aeneus*	AL	De Kalb
UCMVZ 189242	*Aneides*	*Aeneus*	AL	De Kalb
NVPL 6955	*Aneides*	*Ferreus*	OR	Lane
NVPL 6957	*Aneides*	*Ferreus*	OR	Lane
NVPL 6956	*Aneides*	*ferreus*	OR	Lane
NVPL 6958	*Aneides*	*ferreus*	OR	Lane
NVPL 6964	*Aneides*	*ferreus*	OR	Lane
NVPL 6960	*Aneides*	*flavipunctatus*	CA	Mendocino
NVPL 6959	*Aneides*	*flavipunctatus*	CA	
NVPL 6961	*Aneides*	*flavipunctatus*	CA	Mendocino
NVPL 6952-1	*Aneides*	*hardii*	NM	Lincoln
NVPL 6952-2	*Aneides*	*hardii*	NM	Lincoln
NVPL 6963	*Aneides*	*lugubris*	CA	Contra Costa
UCMVZ 189246	*Aneides*	*lugubris*	CA	Santa Clara
UCMVZ 189247	*Aneides*	*lugubris*	CA	Santa Clara
UCMVZ 189248	*Aneides*	*lugubris*	CA	Contra Costa
UCMVZ 189250	*Aneides*	*lugubris*	CA	Contra Costa
UCMVZ 189251	*Aneides*	*lugubris*	CA	Contra Costa
UCMVZ 189255	*Aneides*	*lugubris*	CA	Contra Costa

Table 1 (continued)

UCMVZ 189256	*Aneides*	*lugubris*	CA	Contra Costa	
UCMVZ 189258	*Aneides*	*lugubris*	CA	Contra Costa	
NVPL 6977	*Ensatina*	*eschscholtzii*	CA	Humboldt	
NVPL 6979	*Ensatina*	*eschscholtzii*	CA		
NVPL 6978	*Ensatina*	*eschscholtzii*	CA		
NVPL 6980	*Ensatina*	*eschscholtzii*	CA		
NVPL 6972	*Plethodon*	*elongatus*	CA		
NVPL 6974	*Plethodon*	*elongatus*	CA	Del Norte	
NVPL 6973	*Plethodon*	*elongatus*	CA	Del Norte	
NVPL 6975	*Plethodon*	*dunni*	OR	Lane	
NVPL 6976	*Plethodon*	*dunni*	OR	Lane	
NVPL 6967	*Plethodon*	*neomexicanus*	NM		
NVPL 6968	*Plethodon*	*neomexicanus*	NM	Sandoval	
NVPL 6966	*Plethodon*	*neomexicanus*	NM		
NVPL 6982	*Rhyacotriton*	*variegatus*	OR	Lincoln	
NVPL 6981	*Rhyacotriton*	*variegatus*	OR	Lincoln	
UCMVZ 228722	*Hydromantes*	*shastae*	CA	Shasta	
NVPL 6970	*Hydromantes*	*shastae*	CA	Shasta	
NVPL 6969	*Hydromantes*	*shastae*	CA	Shasta	

Abbreviations: UCMVZ = University of California Museum of Vertebrate Zoology; NVPL = Neogene Vertebrate Paleontology Laboratory, collections housed and excellently curated at East Tennessee State University.

Table 2: Measurements used in this analysis

Abbreviation	Description
PREL	Length between prezygapophyses
POSTL	Length between postzygapophyses
PZL	Length from pre- to postzygapophysis
NAL	Neural arch length
TPL	Transverse process length
TPA	Transverse process angle
CD	Centrum diameter
CL	Centrum length
PPO	Distance between parapophyses

Table 3: Landmarks used in this analysis

Number	Location
1	Dorsal – Midline anterior neural arch
	Posterior – Midline ventral centrum
2	Dorsal – Midline posterior neural arch
	Posterior – Midline dorsal centrum
3	Dorsal – Intersection of centrum and prezygapophysis in photographic plane
	Posterior – Midline ventral neural arch
4	Dorsal – Lateralmost point on prezygapophysis
	Posterior – Midline dorsal neural arch
5	Dorsal – Anterior intersection of transverse process with dorsal neural arch
	Posterior – Tip of hypopophysis
6	Dorsal – Tip of parapophysis
	Posterior – Innermost point on postzygapophysis
7	Dorsal – Tip of diapophysis
	Posterior – Outermost point on postzygapophysis
8	Dorsal – Intersection of hypopophysis with neural arch in photographic plane
	Posterior – Tip of diapophysis
9	Dorsal – Lateralmost point of postzygapophysis
	Posterior – Tip of parapophysis
10	Dorsal – Lateralmost point of hypopophysis
	Posterior – Dorsalmost point of attachment of neural arch to centrum
11	Dorsal – Posteriormost point of hypopophysis
	Posterior – Lateralmost point of attachment of neural arch to centrum

Figure 4 displays the range of size variation. Figure 5 illustrates the locations of measurements on a reference sacrum. Wake (1966) used a pair of vertebral ratios in his analysis of *Aneides* vertebrae: 1) the centrum ratio, defined as the posterior central diameter divided by the centrum length; and 2) the centrum-parapophyseal ratio, defined as the posterior central diameter divided by the distance across the parapophyseal tips. These ratios served to quantify the direction and degree of shape change between species of *Aneides*. This study replicates his measurements in order to test and potentially replicate his results. LaDuke (1991) identified a series of measurements to be used on *Thamnophis* (garter snake) vertebrae, and the study here adapts some of his techniques for use on salamanders. The angle of the transverse process was taken from Babcock and Blais (2001) and modified for use here. Finally, Polly and Head (2004) established a series of landmarks for use on the vertebrae of another snake, *Cylindrophis*, and these landmarks have been adopted for this study by matching the homologous locations on a salamander sacral vertebra.
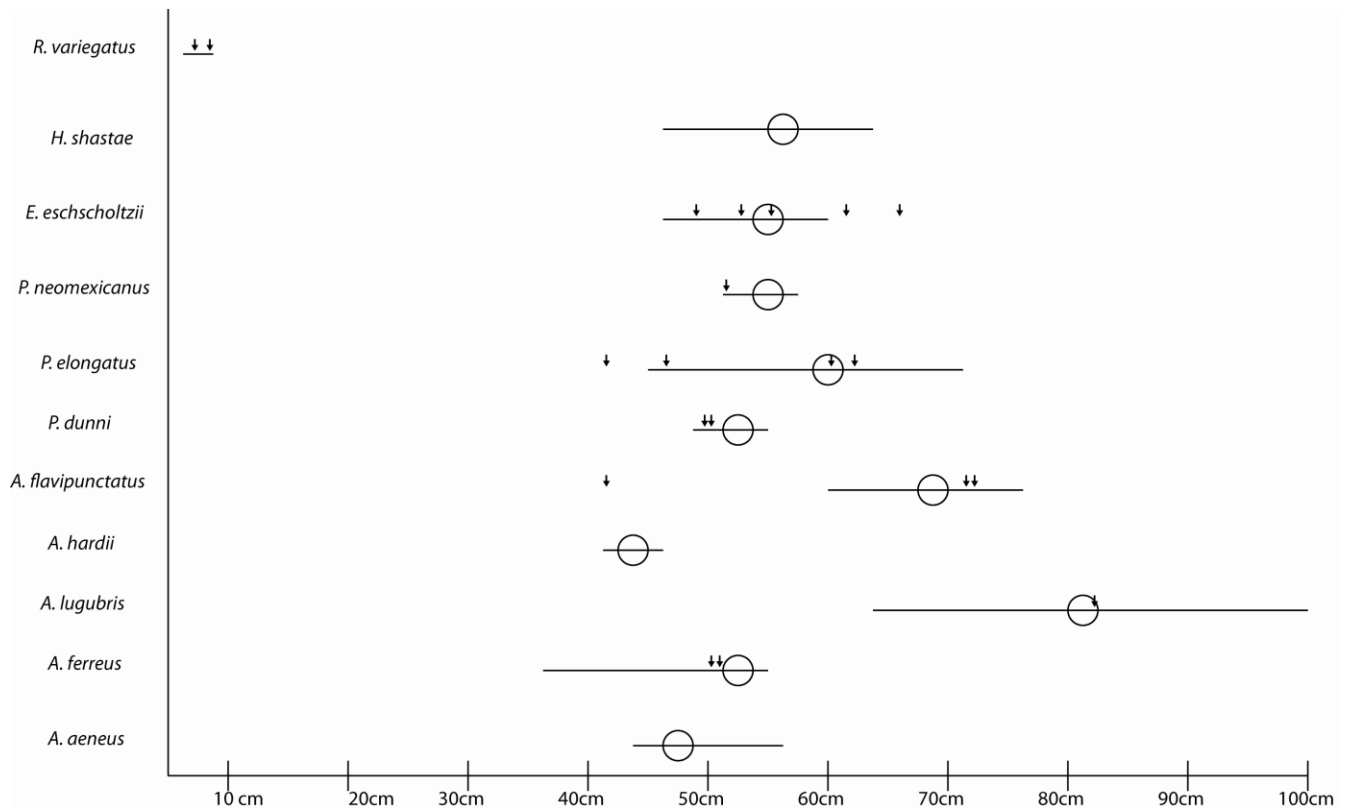
Figure 4: Size data for species average and specimens used in the analysis. Maximum to minimum snout-vent length (svl) of species included in the analysis. Length of line indicates minimum to maximum svl for species (Lanoo 2005, Gorman and Camp 1953). Circles indicate mean svl for species at reproductive maturity (Lanoo 2005, Gorman and Camp 1953). Arrows indicate svl of specimens used in this study; some specimens have no determined svl. R = *Rhyacotriton*, H = *Hydromantes*, E = *Ensatina*, P = *Plethodon*, A = *Aneides*.
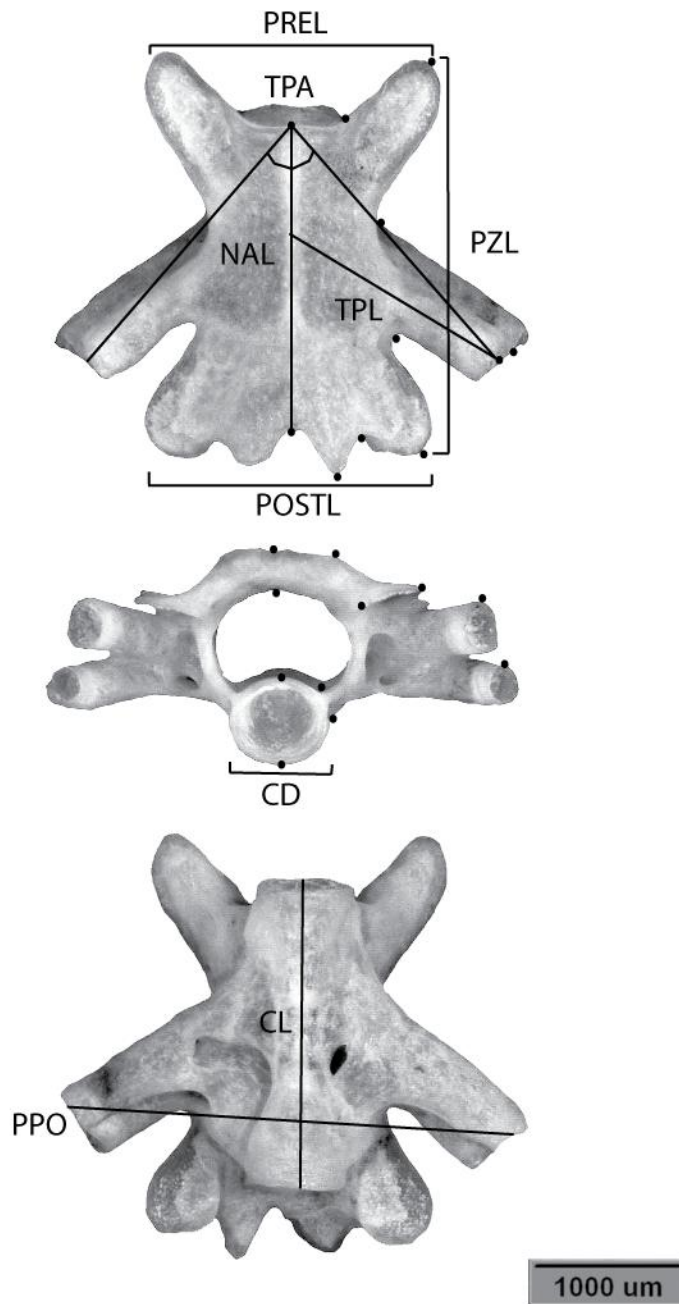
Figure 5: Reference sacra of *Aneides* with measurements and landmarks noted. Reference *Aneides* vertebrae with landmarks and measurements noted. Specimen is *Aneides ferreus* NVPL xxx. PREL = distance between prezygapophyses; PZL = distance from pre- to postzygapophysis; POSTL = distance between postzygapophyses; NAL = neural arch length; TPL = transverse process length; TPA = transverse process angle; CL = centrum length; CD = centrum diameter; PPO = distance between parapophyses. Dots are landmarks.

RESULTS

Qualitative Comparisons

Except where cited, these are qualitative observations of shape change within the set of specimens used in this analysis based on my observations. Reference sacra in dorsal, posterior, and ventral views of *Aneides, Ensatina,* and *Plethodon* can be found in Figure 6. ORCA specimens in dorsal aspect can be found in Figure 7.
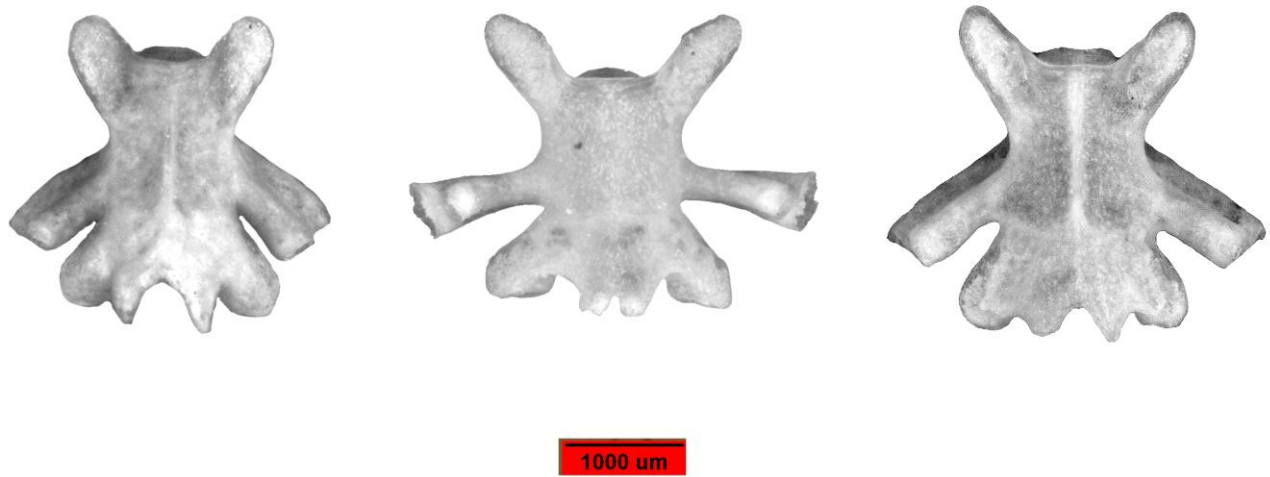

Figure 6: Reference sacra of *Plethodon, Ensatina,* and *Aneides*, in dorsal aspect. Sacral vertebrae in dorsal aspect, oriented with anterior to top. From left to right: *Plethodon, Ensatina, Aneides*.
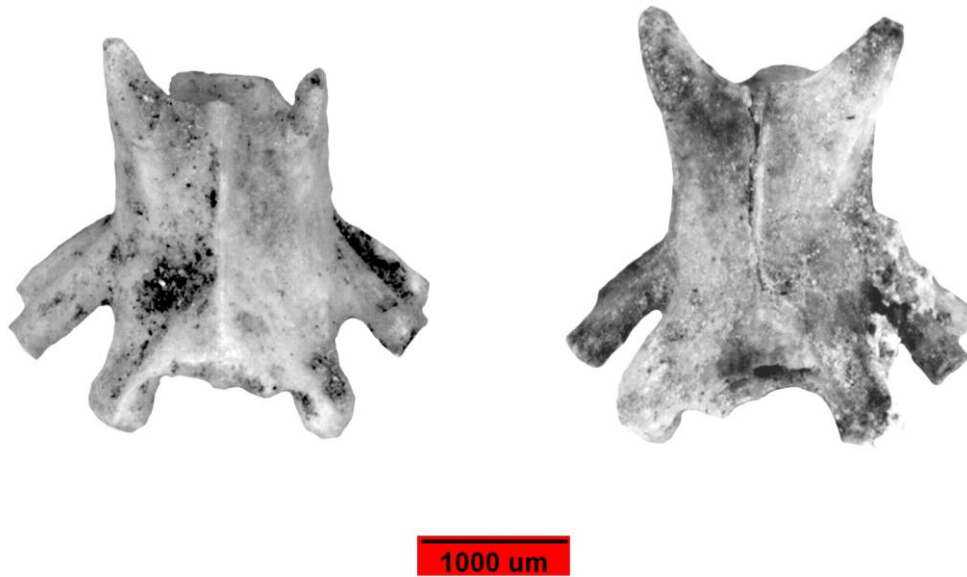
Figure 7: ORCA fossils, in dorsal aspect. Sacral vertebrae from ORCA in dorsal aspect, oriented with anterior to top. From left to right: ORCA 1610, ORCA 1620.

Centrum Structure

Aneides: The centrum of *Aneides* is universally hourglass-shaped, with faint to robust alar processes supporting the transverse processes, which seem to be a distinguishing character of this genus. In ventral aspect, *Aneides aeneus* has both anterior and posterior alar processes of equal size, where *A. ferreus/vagrans*, *A. hardii*, and *A. lugubris* have little to no posterior alar processes but have moderate to large anterior alar processes. *Aneides flavipunctatus* has small anterior and posterior alar processes. In posterior aspect, the centra of *Aneides aeneus* and some specimens of *A. ferreus* are dorsoventrally compressed, giving the centrum an ovoid appearance.

Ensatina/Plethodon: Alar processes are not present in either genus, and the ventral side of the sacrum lacks any distinguishing features in either genus. In posterior aspect, the centra of *Ensatina* are laterally compressed where *Plethodon* centra vary from compressed to elongate.

28

Neural Arch Structure

Aneides: Wake (1966) notes 2 conditions for the hyperapophyses: either 1) they arise united and remain united for the length of the process, or 2) they arise united OR separated -- if the latter, then only on the anterior vertebrae, and they will be separated posteriorly. *Ensatina* and *Hydromantes* have condition 1; all others have condition 2. My own observations of what is admittedly a limited dataset show that in dorsal aspect in *Aneides*, all hyperapophyses separate posteriorly. In *Ensatina*, 2 of 4 specimens have separated hyperapophyses, and in *Hydromantes*, 1 of 2 specimens has separated hyperapophyses. Overall, the hyperapophyses in *Aneides aeneus* are generally flush with the line of the postzygapophysis, whereas in other species of *Aneides* the hyperapophyses extend below the line of the postzygapophysis.

Transverse processes

Aneides: The alar processes of *Aneides* species seem to be the feature that most easily diagnoses them to genus. In ventral aspect, *Aneides lugubris* has the largest and most prominent alar processes anteriorly but little to none posteriorly. Similarly, *Aneides ferreus* and *A. hardii* have anterior alar processes but little to none posteriorly. *Aneides flavipunctatus* has both anterior and posterior alar processes, but these are small in comparison to those of *A. lugubris*. *Aneides aeneus* has well-developed anterior and posterior alar processes. All specimens of *Aneides* examined possess large transverse processes extending well beyond the zygapophyseal/neural arch margins. The tips of both dia- and parapophyses are large and cup shaped. In posterior aspect, the hyperapophyses can vary from flush with the dorsal margin of the neural arch to pronounced humps distinct from the rest of the arch, which is quantifiable as the distance from the dorsalmost point on the neural canal to the dorsalmost point on the neural spine. Overall, the major differences between species of *Aneides* seem to depend on variation in the postzygapophyses, the hyperapophyses, and the degree of flexion or extension of the transverse processes.

Ensatina/*Plethodon:* In dorsal aspect, *Ensatina* transverse processes are almost perpendicular to the rest of the vertebrae and give a very flared appearance. The hyperapophyses vary from flush with to extending below the line of the postzygapophyses, and the prezygapophyses are distinctively long and laterally flared. In contrast, *Plethodon* prezygapophyses are short and stubby and do not flare much laterally. Their hyperapophyses can be long and pointed or short and connected.

<u>Morphometrics</u>

Linear Morphometrics

Figures 8-12 are the results of a series of discriminant analyses of the linear measurements and ratios taken from all specimens included in the study. The taxon that falls out as the most distinct in each analysis will be removed from the next. Figure 8 includes all taxa in the study. Function 1 represents 47% of the variance and distinctly separates *Rhyacotriton variegatus* from the other taxa. Function 2 represents 21% of the variance and separates the remaining taxa from each other. Of the variables included in the analysis, the F-value for Wilks' lambda was highest for the centrum diameter to parapophyseal distance ratio (cd:ppo), and then for the pre- to postzygapophyseal distance to parapophyseal distance ratio (pzl:ppo), neural arch length to pre- to postzygapophyseal distance ratio (nal:pzl), centrum diameter to centrum length ratio (cd:cl), and the transverse process angle (tpa). In this analysis, the ORCA specimens were classified as *A. hardii* (ORCA 1610) and as *Plethodon* sp. (ORCA 1620), which is roughly concurrent with where they have fallen out on the graph. *Rhyacotriton variegatus* were removed from the next analysis to elucidate the relationships between the remaining taxa.

Linear morphometrics

species
- ■ *Aneides aeneus*
- ● *Aneides ferreus*
- ▲ *Aneides flavipunctatus*
- ◆ *Aneides hardii*
- ▼ *Aneides lugubris*
- + *Ensatina eschscholtzii*
- | *Hydromantes shastae*
- − *Plethodon neomexicanus*
- − *Plethodon dunni*
- − *Plethodon elongatus*
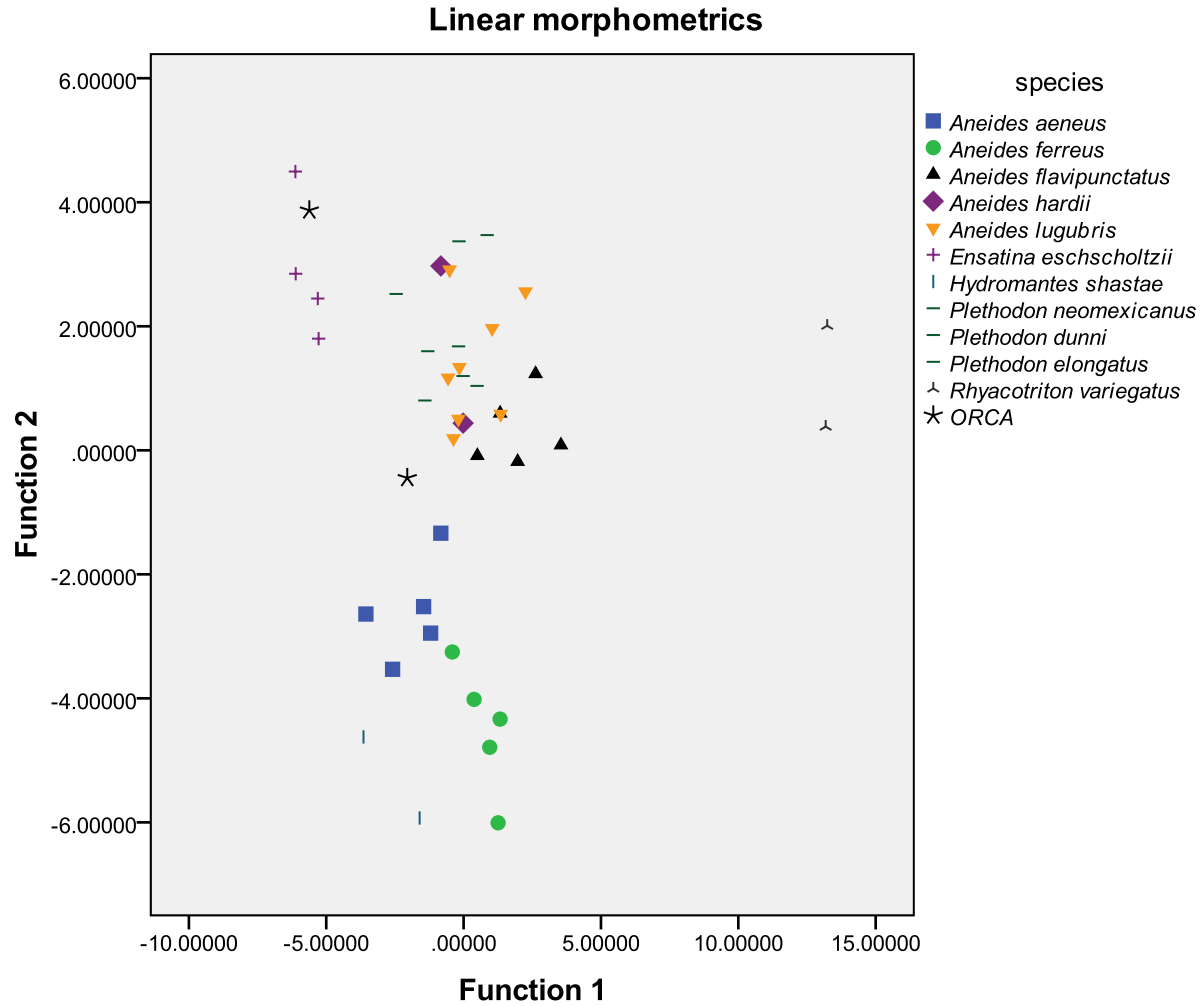- ⋏ *Rhyacotriton variegatus*
- ✶ ORCA

Figure 8: Linear morphometrics, all taxa. Results of a discriminant analysis performed on linear measurements. Dataset includes all taxa listed in the study. Greatest separation occurs along Function 1 from 5.0-10.0. Solid markers indicate *Aneides*: Square = *A. aeneus*, circle = *A. ferreus,* triangle = *A. flavipunctatus*, diamond = *A. hardii,* inverted triangle = *A. lugubris*. Line markers indicate other taxa: Cross = *Ensatina eschscholtzii*, vertical line = *Hydromantes shastae*, dash = *Plethodon* sp., tripod = *Rhyacotriton variegatus*, asterisk = ORCA.

Figure 9 excludes *Rhyacotriton variegatus*. Function 1 represents 47% of the variance and separates a group of taxa including *Hydromantes shastae, A. aeneus*, and *A. ferreus* from the other taxa. Function 2 represents 25% of the variance and separates *Ensatina* from all other taxa. F-values for Wilks' lambda were again highest for the centrum diameter to parapophyseal distance ratio (cd:ppo), followed the centrum length to centrum diameter ratio (cd:cl), the transverse process angle (tpa), and the pre- to postzygapophyseal distance to parapophyseal distance ratio (pzl:ppo). Again, ORCA 1610 was classified as *A. hardii*, and clusters with *Plethodon* sp. on this graph, but ORCA 1620 straddles the 2 groups, even though it is still classified as *Plethodon* sp. As *Ensatina* was the most clearly different, it was removed from the next analysis.
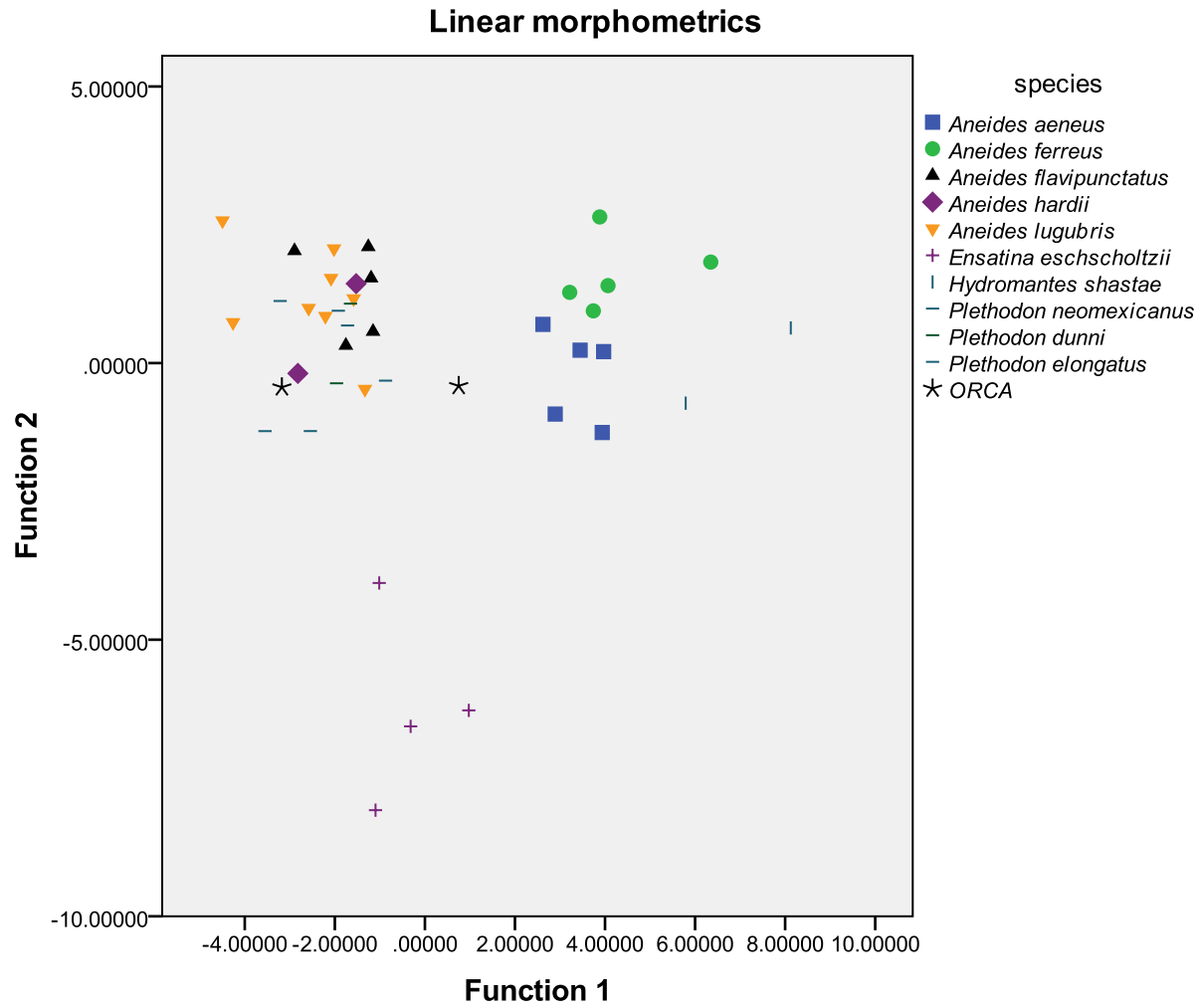
Figure 9: Linear morphometrics, excluding *Rhyacotriton variegatus*. Results of a discriminant analysis performed on linear measurements, excluding *Rhyacotriton variegatus* from the dataset. Solid markers indicate *Aneides*: Square = *A. aeneus*, circle = *A. ferreus*, triangle = *A. flavipunctatus*, diamond = *A. hardii*, inverted triangle = *A. lugubris*.: Line markers indicate other taxa: Vertical line = *Hydromantes shastae*, dash = *Plethodon* sp., asterisk = ORCA.

Figure 10 excludes *Rhyacotriton* and *Ensatina*. Function 1 represents 60% of the variance and separates a group of taxa including *Hydromantes shastae*, *A. aeneus,* and *A. ferreus* from the remaining taxa. Function 2 represents 15% of the variance. There is a clear split in this graph between 2 large groups – the [*H. shastae – A. ferreus – A. aeneus*] group (Group 1), and another group consisting of [*A. lugubris – A. flavipunctatus – A. hardii – Plethodon sp.*] and both ORCA specimens (Group 2). Each group is clustered above 2 separate points along Function 1, and Function 2 serves to separate taxa within groups. F-values for Wilks' lambda remained highest for the centrum diameter to parapophyseal distance ratio (cd:ppo), followed by pzl:ppo, cd:cl, nal:ppo, and tpa. ORCA specimen classifications remained the same, which is congruent with their clustering on the graph. The next two graphs examine in sequence Group 1 and Group 2.

Linear morphometrics
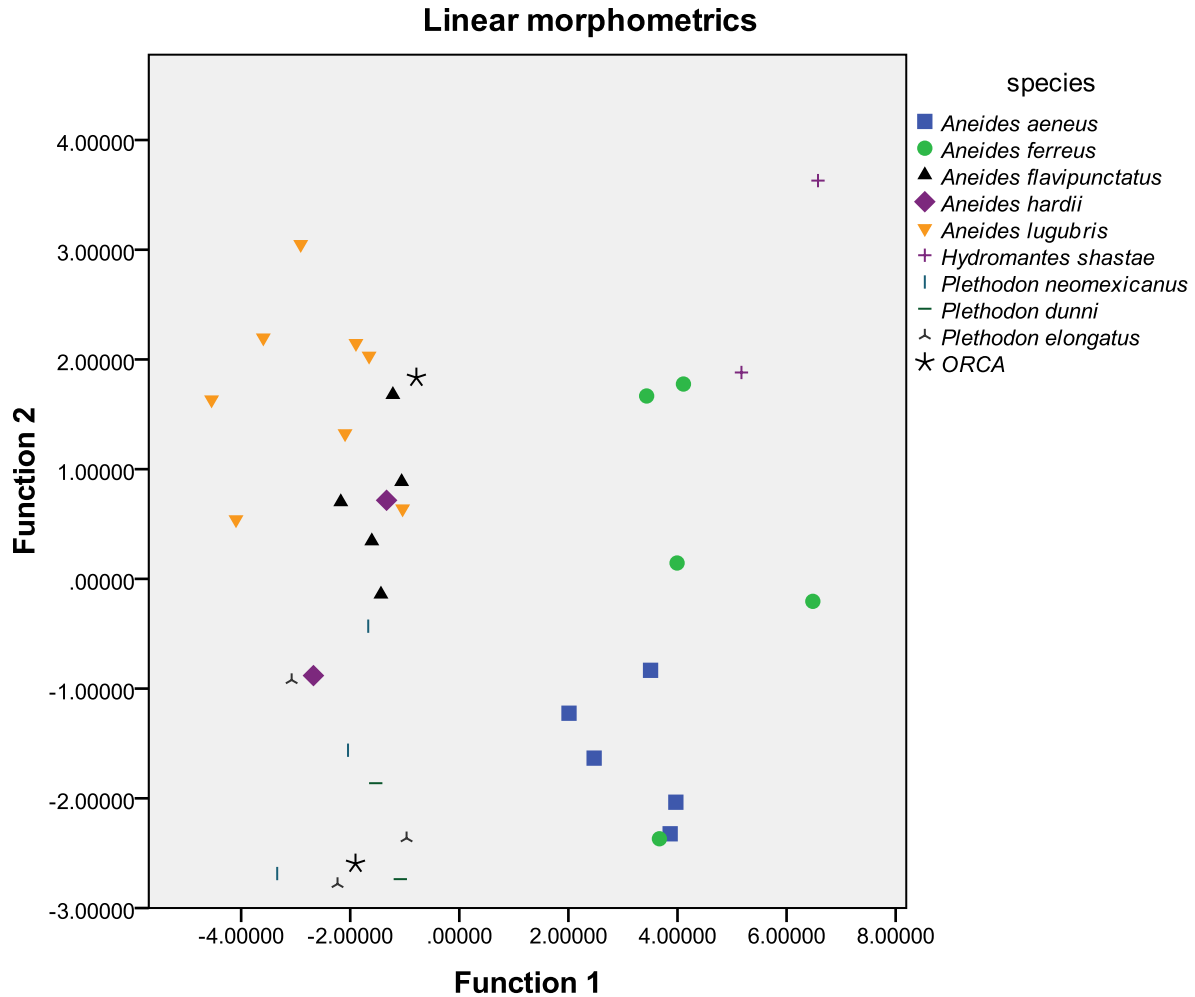
Figure 10: Linear morphometrics, excluding *Rhyacotriton variegatus* and *Ensatina eschscholtzii*. Results of a discriminant analysis performed on linear measurements, excluding *Rhyacotriton variegatus* and *Ensatina eschscholtzii* from the dataset. Greatest separation occurs along Function 1 at 0.0. Solid markers indicate *Aneides*: Square = *A. aeneus*, circle = *A. ferreus,* triangle = *A. flavipunctatus*, diamond = *A. hardii*, inverted triangle = *A. lugubris*.: Line markers indicate other taxa: Vertical line = *Hydromantes shastae*, dash = *Plethodon* sp., asterisk = ORCA.

Figure 11 includes only *A. aeneus, A. ferreus,* and *Hydromantes shastae*, the Group 1 from the previous graph (Figure 10). Function 1 represents 93% of the variance, and Function 2 represents 6% of the variance. The most discriminating variable for this analysis was the centrum diameter according to the f-values for Wilks' lambda.

Linear morphometrics
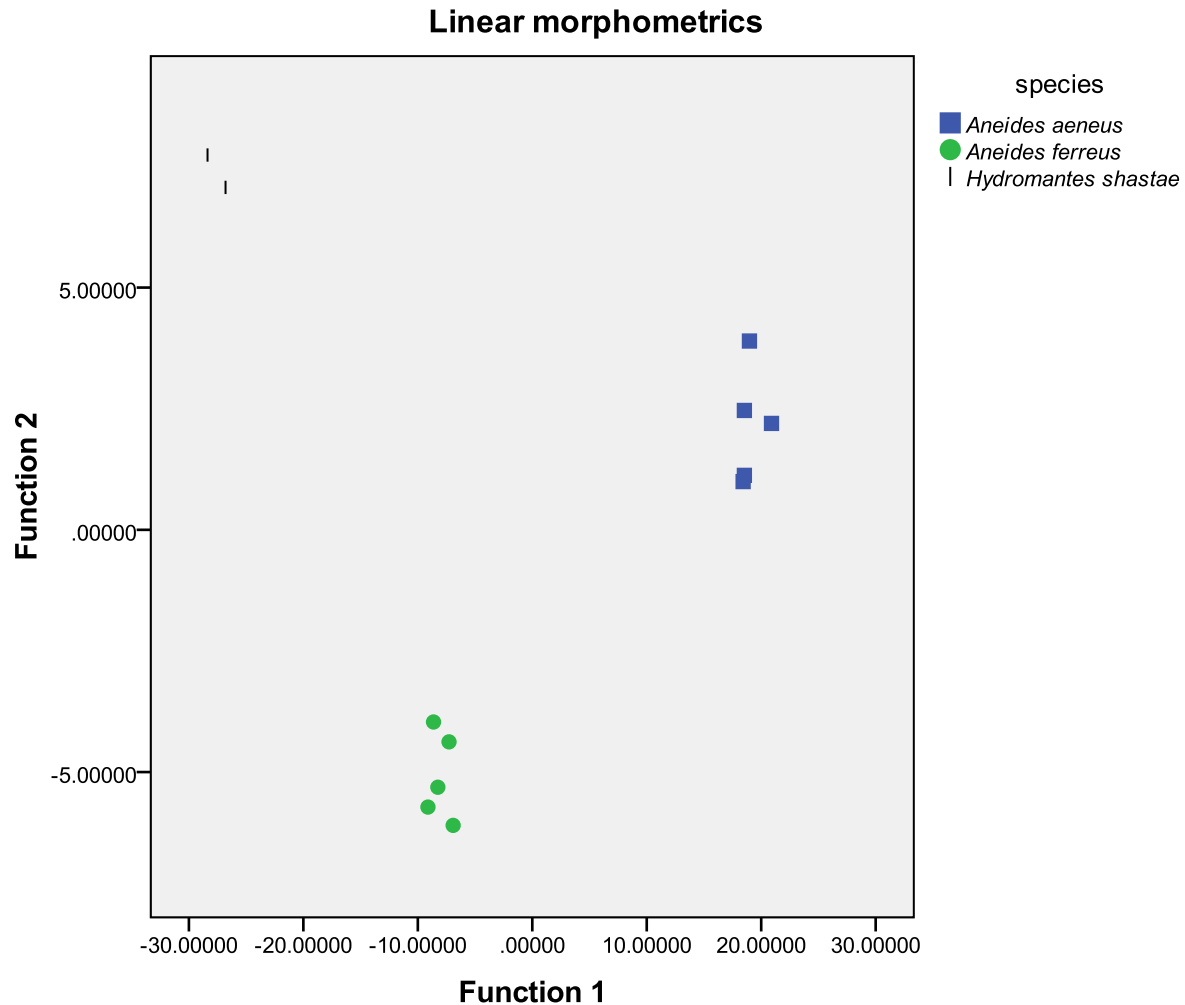

Figure 11: Linear morphometrics, Group 1 (*Aneides ferreus, Aneides aeneus,* and *Hydromantes shastae*). Results of a discriminant analysis performed on the linear measurements taken from the first group from Figure 11. Solid markers indicate *Aneides*: Square = *A. aeneus*, circle = *A. ferreus.* Line markers indicate other taxa: vertical line = *Hydromantes shastae*.

Figure 12 includes only *A. flavipunctatus, A. hardii, A. lugubris, P. neomexicanus, P. dunni, P. elongatus,* and the ORCA specimens. Function 1 represents 83% of the variance, whereas Function 2 represents only 11%. The overall distribution is shotgun and thus not clear enough to continue removing taxa, but Function 1 seems to separate the *Plethodon* taxa from the *Aneides* taxa. The ORCA specimens, which are still classified as *A. hardii* (1610) and *Plethodon sp.* (1620), fall out as clear outliers on the graph, but 1610 is on the *Aneides* side of the graph, whereas 1620 is on the *Plethodon* side of the graph.
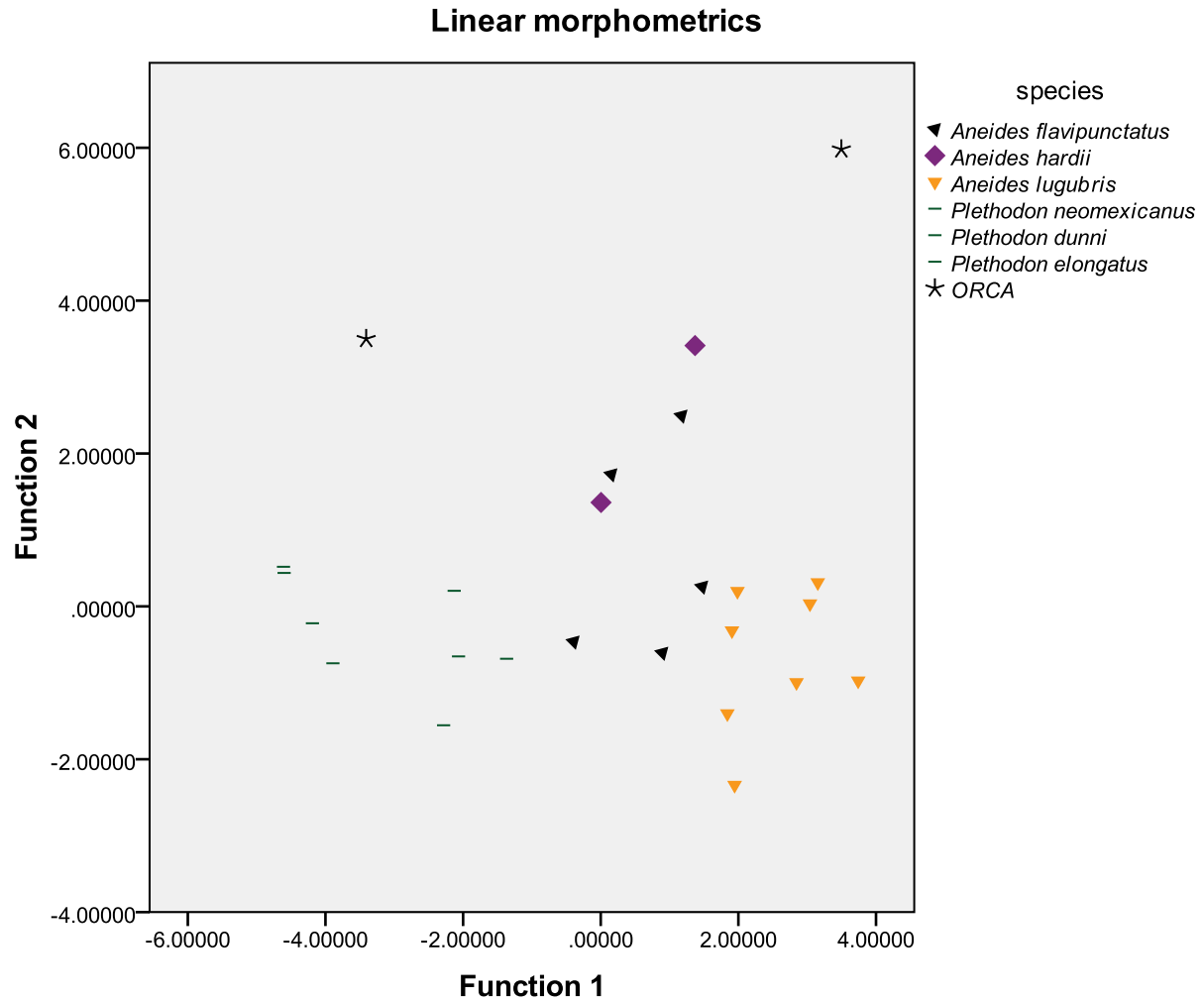
Figure 12: Linear morphometrics, Group 2 (*Aneides flavipunctatus, Aneides hardii, Aneides lugubris, Plethodon neomexicanus, Plethodon dunni, Plethodon elongatus,* and ORCA fossils. Results of a discriminant analysis performed on the linear measurements taken from the second group from Figure 11. Solid markers indicate *Aneides*: triangle = *A. flavipunctatus*, diamond = *A. hardii*, inverted triangle = *A. lugubris*.: Line markers indicate other taxa: dash = *Plethodon* sp., asterisk = ORCA.

Geometric Morphometrics

Figures 13-19 are the results of a series of discriminant analyses of the dorsal Procrustes landmarks of all specimens included in the study and the thin-plate splines produced by plotting the Procrustes landmarks associated with each taxon. Again, the taxon that falls out as most distinct will be removed from subsequent analyses.

Figure 13 includes all taxa. Function 1 represents 32% of variance, and Function 2 represents 24%. The clearest separation on this graph is between *Ensatina* and all other taxa, but a reasonable argument could be made for the ORCA specimens and *Rhyacotriton* as a separate, equally-distinct group. In contrast to the results of the linear measurements (Figures 8-12), the ORCA specimens were both classified as *Hydromantes*, but they are associated with *Rhyacotriton* on the graph. F-values for Wilks' lambda were highest for Y2 and X5, which seem to correspond to the posterior neural arch and the angle of the transverse processes, respectively. As the object of this study is to examine the possible identifications of ORCA specimens, their group will remain but *Ensatina* was removed from the next analysis.

Dorsal Procrustes coordinates
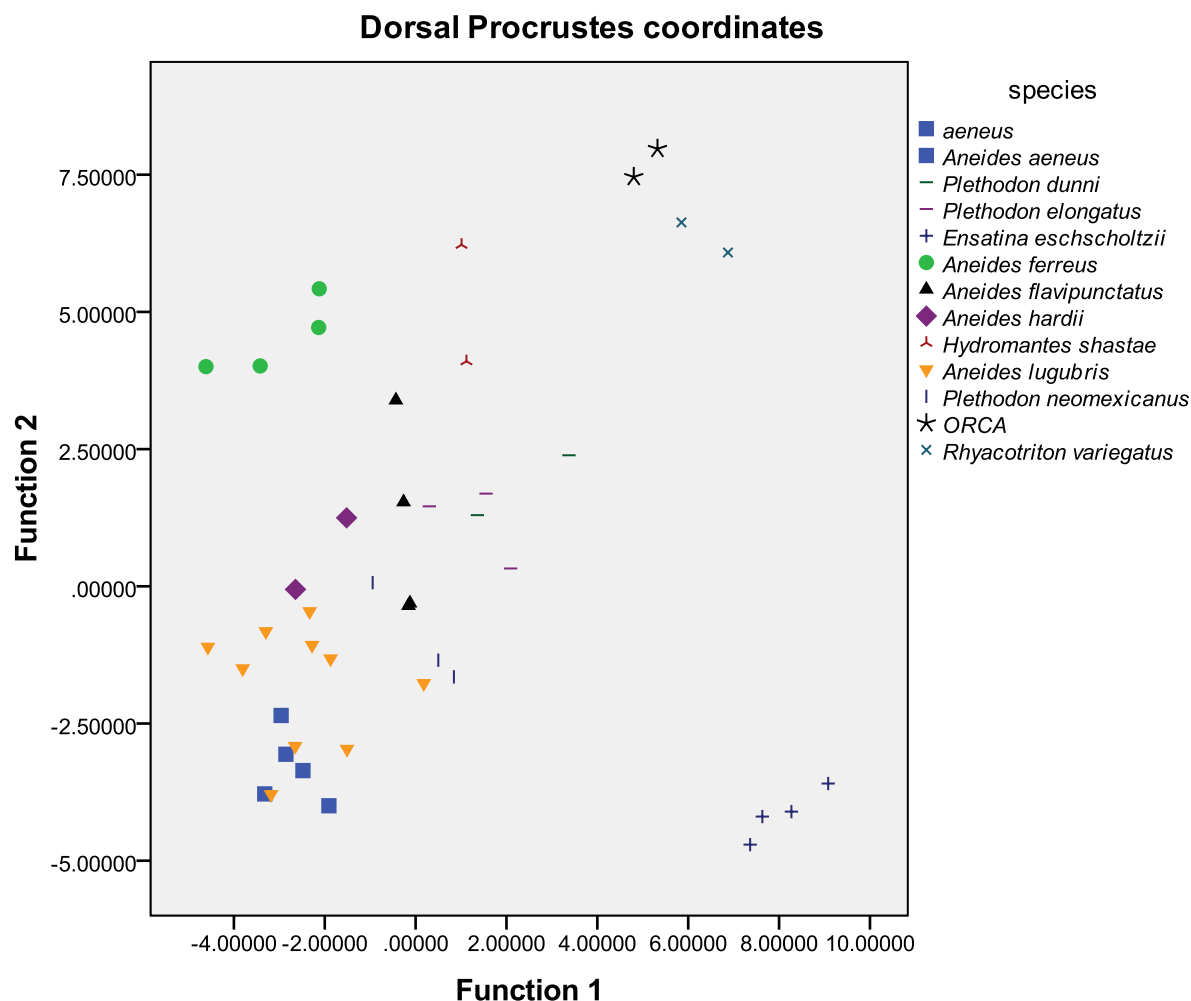
Figure 13: Geometric morphometrics – dorsal Procrustes, all taxa. Results of a discriminant analysis performed on the procrustes coordinates from the dorsal landmarks of all taxa included in the study. Greatest separation among taxa occurs along 4.0 on Function 1; secondary separation between *Ensatina eschscholtzii,* and *Rhyacotriton variegatus* and ORCA fossils, along Function 2. Solid markers indicate *Aneides*: Square = *A. aeneus*, circle = *A. ferreus,* triangle = *A. flavipunctatus*, diamond = *A. hardii*, inverted triangle = *A. lugubris*.: Line markers indicate other taxa: Cross = *Ensatina eschscholtzii*, vertical line = *Hydromantes shastae*, dash = *Plethodon* sp., tripod = *Rhyacotriton variegatus*, asterisk = ORCA.

Figure 14a is a thin-plate spline of a combination of the ORCA specimens and *Rhyacotriton* because these specimens grouped together on the graph in Figure 13. The greatest deformation on this spline occurs near the posterior of the vertebrae. Figure 14b is a thin-plate spline of *Ensatina,* the other group that was separated from the main cluster in Figure 13. Most deformation in this spline occurs in the area where the tranverse processes attach to the centrum itself.
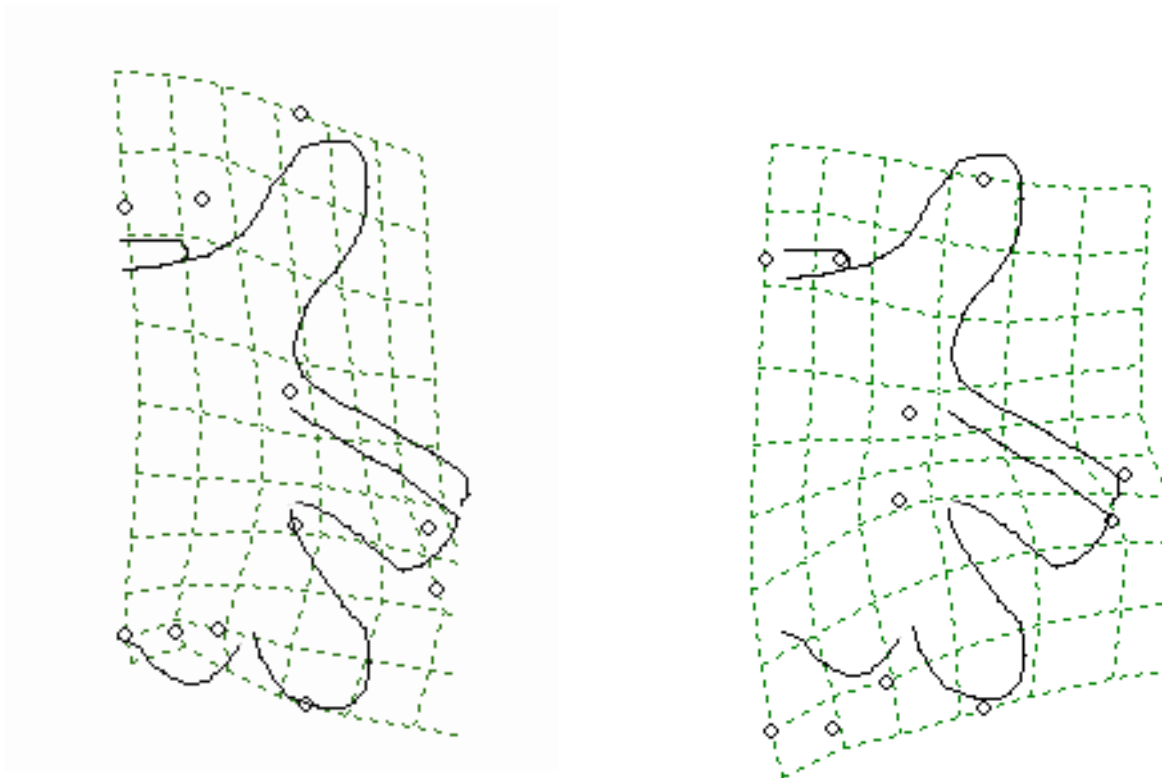
Figure 14: Thin plate splines for Figure 13 – a) ORCA + *Rhyacotriton variegatus,* b) *Ensatina eschscholtzii*. Thin-plate splines from dorsal Procrustes coordinates, representing deformation in the analysis depicted in Figure 15. Areas that are "warped" represent the degree and direction of deformation from the consensus. The drawn sacral represents a consensus of all taxa included in the analysis. Figure a) represents the ORCA specimens

Figure 15 excludes *Ensatina* from the analysis. Function 1 represents 36% of the variance, and Function 2 represents 22%. As in Figure 13, ORCA specimens are classified as *Hydromantes*, and the most significant variables are once again Y2 and X5, the landmarks located on the posterior neural arch and the transverse processes. The clearest grouping is the cluster of *Hydromantes, Rhyacotriton* and ORCA, and the remaining taxa cluster along Function 1. Again, as the aim of this study is to identify the ORCA specimens, a discriminant analysis performed containing only the ORCA specimens plus *Rhyacotriton* and *Hydromantes* classifies both ORCA specimens as *Rhyacotriton* and returns only one function that explains 100% of the variance.

Dorsal Procrustes coordinates

species
- ■ *aeneus*
- ■ *Aneides aeneus*
- ─ *Plethodon dunni*
- ─ *Plethodon elongatus*
- ● *Plethodon ferreus*
- ▲ *Aneides flavipunctatus*
- ◆ *Aneides hardii*
- | *Hydromantes shastae*
- ▼ *Aneides lugubris*
- ─ *Plethodon neomexicanus*
- ✱ *ORCA*
- × *Rhyacotriton variegatus*
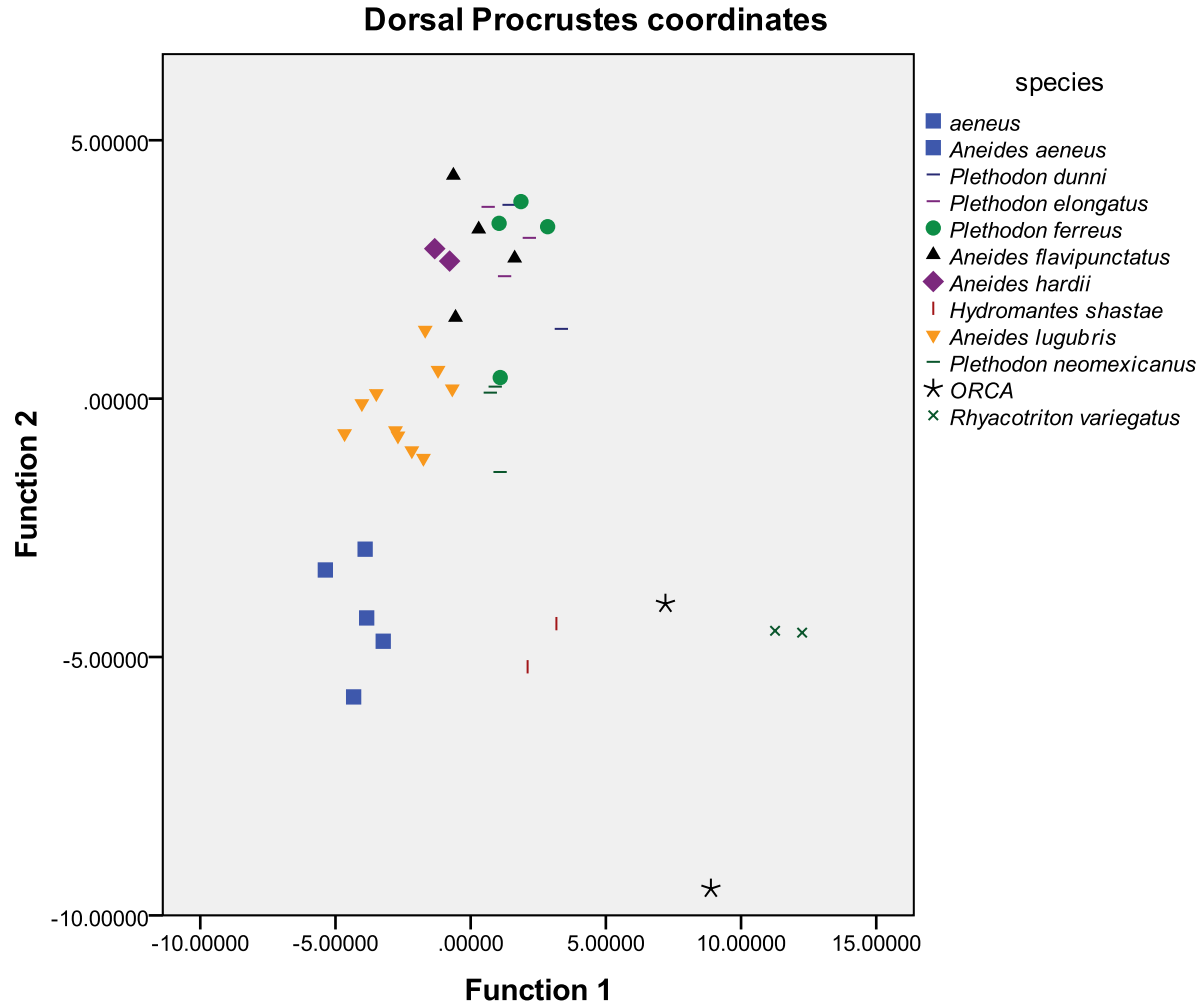
Figure 15: Geometric morphometrics – dorsal Procrustes, excluding *Ensatina eschscholtzii*. Results of a discriminant analysis performed on the dorsal Procrustes coordinates of selected taxa. *Ensatina eschscholtzii* has been excluded from this analysis. Greatest separation occurs along Function 1 at 0.0 – 5.0. Solid markers indicate *Aneides*: Square = *A. aeneus*, circle = *A. ferreus,* triangle = *A. flavipunctatus*, diamond = *A. hardii*, inverted triangle = *A. lugubris*.: Line markers indicate other taxa: Vertical line = *Hydromantes shastae*, dash = *Plethodon* sp., tripod = *Rhyacotriton variegatus*, asterisk = ORCA.

Figure 16a is the thin-plate spline of *Hydromantes, Rhyacotriton,* and the ORCA specimens.

Most deformation in this figure occurs at the tips of the transverse processes and the posterior edge of

the neural arch. This is similar to the results of the DA from Figure 15, where the 2 most significant

landmarks were located on the posterior neural arch and the transverse processes. Figure 16b is the

thin-plate spline of *Aneides aeneus*, the other taxon to be separated from the main cluster by Function

1. Again, most bending energy in this figure occurs around the transverse processes and posterior

margins.
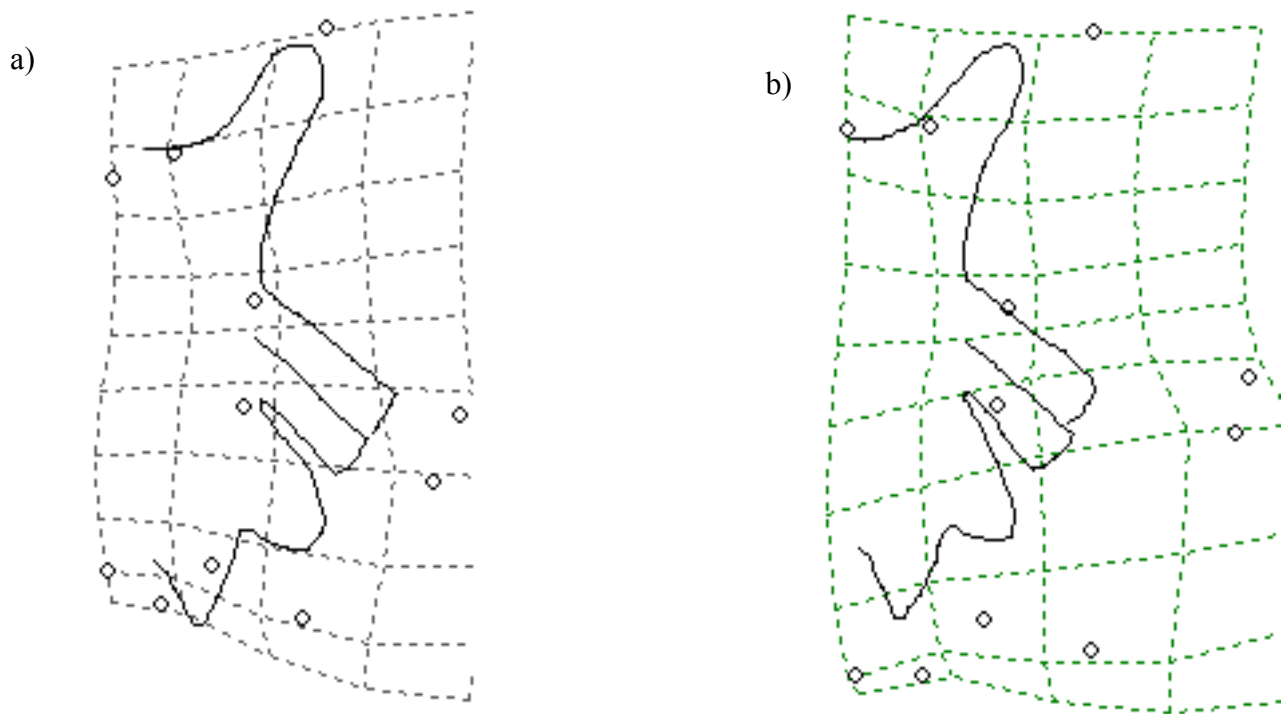
Figure 16: Thin plate splines for Figure 15 – a) *Aneides aeneus*, b) ORCA + *Rhyacotriton variegatus* + *Hydromantes shastae*. Thin-plate splines from dorsal Procrustes coordinates, representing deformation in the analysis depicted in Figure 14. Areas that are "warped" represent the degree and direction of deformation from the consensus. The dark outline represents the consensus of all taxa included in this analysis here. Figure a) represents the ORCA specimens, *Hydromantes shastae* and *Rhyacotriton variegatus*. Figure b) represents *Aneides aeneus*.

Figure 17 includes only *Plethodon* and *Aneides* species. Most taxa cluster around .000 on Function 1, which makes up 49% of the variance. Function 2 contributes 32% of variance and separates within this large cluster, bringing *A. ferreus* out as the most distinct taxon. However, the variation exhibited by *A. flavipunctatus* and *A. hardii* precludes its removal from any subsequent analyses. Additionally, the variation in *A. hardii* places it too close to the *Plethodon* group to be able to remove *Plethodon* sp., thus stopping the discriminant analysis series here. F-values for Wilks' lambda were highest again for Y2, Y5, and X3, all variables associated with posterior landmarks.

Dorsal Procrustes coordinates
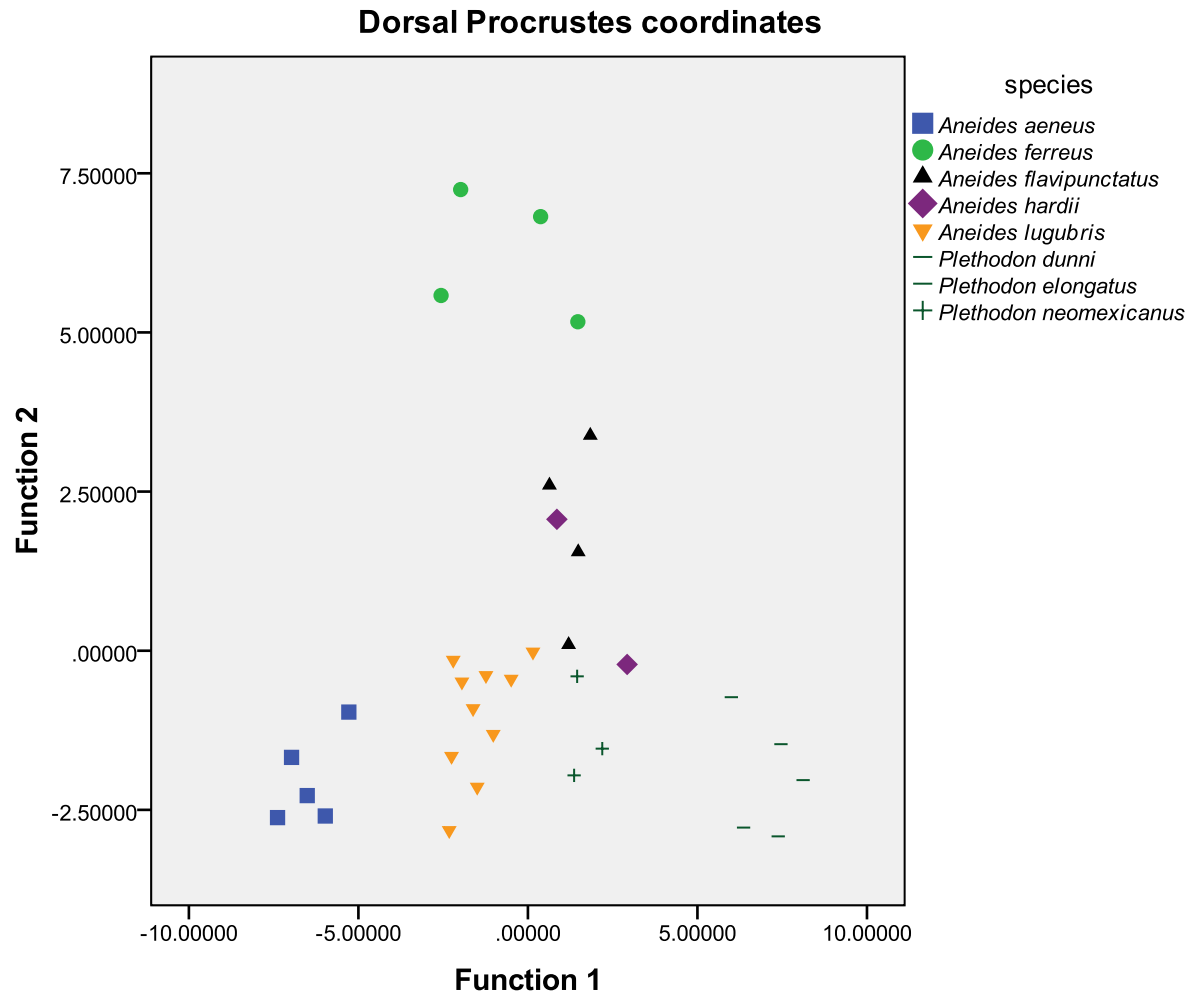
Figure 17: Geometric morphometrics – dorsal Procrustes, excluding *Ensatina eschscholtzii, Hydromantes shastae, Rhyacotriton variegatus*, and ORCA fossils.
Results of a discriminant analysis performed on the dorsal Procrustes coordinates of selected taxa. *Ensatina eschscholtzii, Hydromantes shastae, Rhyacotriton variegatus* and the ORCA specimens have been excluded from this analysis. Greatest separation occurs along Function 2 at 5.0. Solid markers indicate *Aneides*: Square = *A. aeneus*, circle = *A. ferreus*, triangle = *A. flavipunctatus*, diamond = *A. hardii*, inverted triangle = *A. lugubris*. Line markers indicate other taxa: dash = *Plethodon* sp.

Figure 18a is the thin-plate spline of *Aneides ferreus*, the only distinctly separate group in that analysis. Again, most deformation occurs towards the posterior of the sacrum, but this taxon seems to have extended its sacrum anteroposteriorally and flexed the transverse processes towards the posterior.
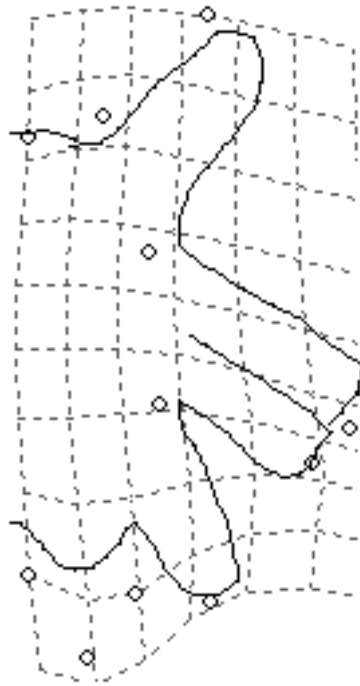
a)

Figure 18: Thin plate splines for Figure 17 – a) *Aneides ferreus*. Thin-plate splines from dorsal Procrustes coordinates, representing deformation in the analysis depicted in Figure 19. Areas that are "warped" represent the degree and direction of deformation from the consensus. The outline represents a consensus of all taxa included in this analysis. Figure a)

Figure 19 is the results of the only successful discriminant analysis performed on the posterior Procrustes coordinates of all taxa included in the study. Again, the distribution is more similar to a shotgun blast than anything meaningful. Most taxa cluster in the center of the graph even though Function 1 contributes 62% and Function 2 contributes 22% of variance. *Rhyacotriton* and *Hydromantes* are the only taxa to be separated from the main cluster but are roughly equal in difference from the main cluster. ORCA 1610 is classified as *A. flavipunctatus* and ORCA 1620 is classified as *Ensatina*. F-values for Wilks' lambda are highest for X2, followed by X4, Y5, Y6, and Y7. This analysis ends here, as there is no clear direction in which to proceed.
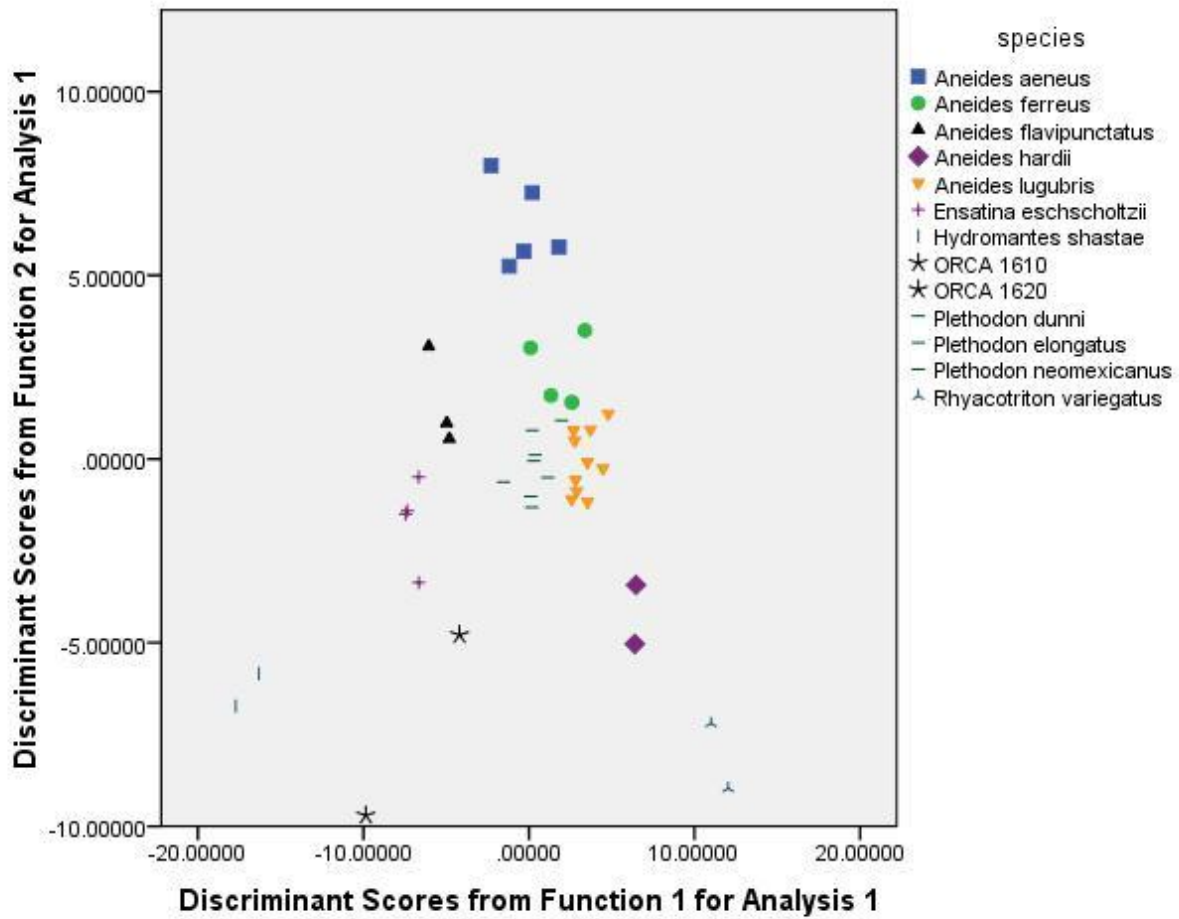
Figure 19: Geometric morphometrics – posterior Procrustes, discriminant analysis, all taxa. Results of a discriminant analysis of the posterior Procrustes coordinates from all taxa included in this study. Little if any separation occurs along any axis. Solid markers indicate *Aneides*: Square = *A. aeneus*, circle = *A. ferreus,* triangle = *A. flavipunctatus*, diamond = *A. hardii*, inverted triangle = *A. lugubris*.: Line markers indicate other taxa: Cross = *Ensatina eschscholtzii*, vertical line = *Hydromantes shastae*, dash = *Plethodon* sp., tripod = *Rhyacotriton variegatus*, asterisk = ORCA.

CHAPTER 4

DISCUSSION

This study had 2 goals: First, to compare and test qualitative comparisons, traditional

morphometrics, and geometric morphometrics as ways to analyze shape change in the sacral vertebra

of *Aneides* salamanders. Qualitative analysis and linear measurements are the traditional methods of

assessing osteological shape change, but geometric morphometrics is a relatively new method that has

not yet been used on sacral vertebrae in salamanders, thus any comparison between the 2 methods will

certainly reveal advantages and drawbacks. Second, this study diagnosed fossil salamander specimens

from ORCA, which was a real-life test to check the methodology and point out advantages, drawbacks,

and provide a possible direction for future research. The most successful method of distinguishing one

species group from another in either the traditional or geometric morphometrics analyses was to use a

discriminant function analysis where all variables are considered together instead of evaluated

separately for their individual contributions. A stepwise discriminant analysis, where variables are

added and removed in a stepwise fashion in the analysis, was unable to distinguish between any of the

groups. This indicates a combination of variables, not one or two in particular, served to discriminate

best between species.

Overall, the combination of these 2 approaches made it possible to draw meaningful

comparisons between methods, as certain characters proved to be significant in each analysis. As the

thin-plate splines (Figures 14, 16, and 18) demonstrated, the degree of transverse process flexion away

or compression towards the body of the vertebra was a distinguishing character for *A. ferreus* and *A.*

aeneus, for example, as was the size of the alar processes. Interpreting the results of each discriminant

analysis in the light of these distinct characters was thus successful in the sense that each species

analyzed fell out as distinct from the others in a meaningful way. Consequently, making the cognitive

50

leap from "known" to "unknown" was fairly simple, as an "unknown" fossil specimen could be entered into the analysis with the expectation of at least a generic-level identification.

<center>Morphometric Analyses</center>

Most analyses, especially as more and more taxa were removed from each analysis, were able to cluster groups according to phylogeny. In the first discriminant analysis from the linear morphometrics (Figure 8), *Rhyacotriton* is separated from the rest of the taxa by Function 1, which was most closely associated with the ratio of the centrum diameter to the distance between the parapophyses. This separation is congruent with the phylogenies provided by both Mueller et al. (2004) and Chippendale et al. (2004). The results from the discriminant analysis of the dorsal Procrustes landmarks suggest a similar pattern (Figure 13), with *Rhyacotriton variegatus* and the ORCA fossils separated from the other taxa by Function 1. However, when *Rhyacotriton* is removed from the analysis, subsequent discriminant functions (Figures 8 and 13) tend to select *Ensatina eschscholtzii* as "more different" from the other taxa, when both Mueller et al. (2004) and Chippendale et al. (2004) place *Ensatina* as a sister group to *Aneides* (Figures 1 and 2). The thin-plate splines from Figure 13 show that for *Ensatina,* most deformation is occuring at the junction of the transverse processes and the centrum, which is congruent with the linear morphometrics that indicated the discriminant function was most heavily influenced by the ratio between the centrum diameter and the distance between the parapophyses and to a smaller extent by the angle of the transverse processes. These results are similar to those of other researchers (Olori and Bell, pers. comm.) in that traditional phylogenies and phyletic analyses fall apart at higher taxonomic levels but retain their integrity at the specific or subspecific levels. However, these results are contrary to those of Wake (1966) and Chippendale et al. (2004), who noted that osteological identification is easy at higher taxonomic levels, but more difficult for species-level identification.

Consistently, the factors contributing the most to each function included variables relating to the

<center>51</center>

length and width of the sacrum and to the position and length of the transverse processes. In the traditional morphometrics analyses the ratio of the centrum diameter to the distance between the parapophyses is taken directly from Wake (1966), as he identified it as a useful distinguishing character, and these results support that conclusion. Other variables important to the analyses measured the spread of the prezygapophyses or postzygapophyses and the relative flexion and extension of the transverse processes. By including ratios of these measurements, the analyses essentially bootstrapped the dataset by resampling some of the data. While this may not be common practice, the small size of the dataset and the fact that previous work (Wake, 1966) has used ratios to distinguish between salamander species justified its use here. In the geometric morphometric analyses, each discriminant function consistently showed that the dominant function was composed of landmarks closer to the posterior end of the sacrum.

Within *Aneides*, *A. hardii*, *A. flavipunctatus,* and *A. lugubris* consistently plotted together in either the linear or dorsal Procrustes morphometrics analyses to the exclusion of *A. aeneus* and *A. ferreus*. In Figure 12, some *Aneides* species plus the *Plethodon* species were analyzed separately to examine their relationships more closely. While the discriminant function was able to distinguish between *Plethodon* and *Aneides* species, the separation was not significant enough to permit further analysis. Another interesting result to note is that *A. aeneus* and *A. ferreus* consistently plotted together in the discriminant analyses of the linear morphometrics, but the results from the dorsal Procrustes analyses were not able to replicate this relationship.

<div align="center">ORCA Fossils</div>

The ORCA fossils (Figure 7) were initially identified as „Caudata' by Sandra L. Swift (pers. comm.). In my study here, I have identified them as sacral vertebrae based on their relatively enlarged transverse processes. A principal components analysis was performed that was unable to distinguish

any meaningful groupings among the included taxa. A PCA is designed to condense multiple axes of variability into 2 major axes of coefficients of variability, and the fact that it was unable to do so here suggests that a combination of factors, and not just 1 or 2 major axes of variance, contribute to the morphological differences between species. However, the discriminant analyses were able to separate taxa into coherent groups and then assign the ORCA specimens a placement on the graph based on the degree of similarity to one group or another. The linear morphometrics analysis (Figure 12) suggested that the ORCA specimens were most similar to either *Plethodon* or *Aneides*, yet in contrast, the data presented by the dorsal Procrustes analysis (Figure 15) suggest that these fossils are most similar to either *Rhyacotriton* or *Hydromantes*.

The results from my research provide 4 possible conclusions about the identifications of the two ORCA fossils. Based on the morphometric analyses, I would not assign either of these specimens to *Plethodon* or *Aneides*, although these identifications are supported by the linear morphometrics. Based on the qualitative analyses and supported by most of the dorsal morphometrics, I would guardedly assign both specimens to *Hydromantes* based on the 1) elongate but wide neural arch, 2) the enlarged but short and widely offset transverse processes, and 3) the straight, unflared pre- and postzygapophyses. Figure 16b is the thin-plate spline formed by a consensus of *Rhyacotriton, Hydromantes,* and the ORCA fossils, and its deformation is most concentrated along the outer edges - at the tip of the prezygapophysis, the tips of the transverse processes, and the posterior neural arch and postzygapophysis, but upon visual examination of the fossils and comparison with known specimens, they are most similar to *Hydromantes*.

Each of these identification options offer interesting implications. ORCA is situated in the Siskyou Mountains of Oregon, bridging the gap between the Sierra Nevada and the Cascades. This would be an ideal place for salamanders to pass through on their way up the Oregon coastline, as its cool and humid habitat would be suitable for plethodontid movement. If the fossils are indeed *Plethodon* or *Aneides*, it

would represent a new locality for the fossil history of both these genera and some time depth to their existence in the western coast of North America. If, as the dorsal morphometrics suggest, these specimens are *Rhyacotriton*, this would be the first fossil record for this genus. Finally, and perhaps most interestingly (and the one preferred here), if the fossils are *Hydromantes*, their presence in the fossil record at ORCA suggests that the range of *Hydromantes* was at one point larger, with a more northward extension, and has only recently contracted to its present (and possibly relictual) state; this would also only be the second fossil record of the genus. Of the salamander fossils available from ORCA, these 2 specimens were the only sacral vertebrae out of over 200 trunk vertebrae collected and identified. Clearly, there is much to learn here.

<u>Conclusions</u>

This work provides the first steps in identifying fossil salamander vertebrae with some statistical confidence. My first goal was to assess whether or not morphological variation can be seen in the sacral vertebrae of salamanders and to compare and contrast the ability of traditional and geometric morphometric techniques to define that variation. This study has shown that regardless of the metric used, morphological variation can be seen in the sacral vertebrae of salamanders. It seems that while qualitative assessment is a good starting point, much promise lies with linear and geometric morphometrics as a way to quantify shape variation. While confident diagnosis to species level is not possible at this time, the techniques presented here, when combined with a more robust database of morphometric data could indeed help identify sacral vertebrae to species. Second, this study used fossil salamander sacral vertebra from Oregon Caves National Monument (ORCA) as a test to see how these assumptions worked when applied to the fossil record. Again, while statistically-supported diagnosis was a bit out of reach at this time, the data suggest great promise for these techniques.

Traditional qualitative identifications have produced a vast body of work so far, and it would be

rash to put that aside in favor of a morphometric method, but as this study has shown using both methodologies can reveal new perspectives on fossil material. Although at this stage it is difficult to assign identifications at any level higher than the generic with great statistical confidence, this is most easily remedied by the addition of more linear and landmark data from other *Aneides* specimens and from other salamanders within Plethodontidae. Clearly, the most immediate need is for a more comprehensive comparative collection to add to the present database; an ontogenetic series is mandated. In lieu of more specimens, though, it would be interesting to try to combine all 3 datasets using the "common language" of Thiele's (1993) continuous-character coding strategy. Coding all these characters for all these taxa by hand would be time-consuming but could possibly tie the scraps of morphological data into a cohesive and robust dataset. Another strategy might be to use geometric morphometrics on the pelvic girdles of articulated specimens and include data about attachment angles and joint loading, but articulated osteological specimens are hard to come by, and finding enough to make a robust dataset would be difficult and would likely require extensive collection. With the current decline in amphibian populations (Lannoo, 2005), collection of live specimens may not be feasible.

REFERENCES

Adams DC. 2004. Character displacement via aggressive interference in Appalachian salamanders. Ecology 85:2664-2670.

Babcock SK, and Blais JL. 2001. Caudal vertebral development and morphology in three salamanders with complex life cycles (*Ambystoma jeffersonianum, Hemidactylium scutatum,* and *Desmognathus ocoee*) J Morph 247:142-159.

Bookstein FL. 1997. Morphometric tools for landmark data: geometry and biology. Cambridge: Cambridge University Press. 435 p.

Chippindale PT, Bonett RM, Baldwin AS, and Wiens JJ. 2004. Phylogenetic evidence for a major reversal of life-history evolution in plethodontid salamanders. Evolution 58:2809-2822.

Christiansen P. 2008. Species distinction and evolutionary differences in the clouded leopard (*Neofelis nebulosa*) and Diard's clouded leopard (*Neofelis diardi*). J Mamm 89:1435:1446.

Duellman WE, and Sweet SS. 1999. Distribution patterns of amphibians in the Nearctic region of North America In: Duellman WE, editor. Patterns of distribution of amphibians: a global perspective. Baltimore: Johns-Hopkins Press. p 31-109.

Dunn ER. 1926. The Salamanders of the Family Plethodontidae. Northampton: Smith College.

Estes R, and Baez A. 1985. Herpetofaunas of North and South America during the late Cretaceous and

    Cenozoic: evidence for interchange? *In* Stehli FG and Webb DS, editors. The Great American

    Biotic Interchange. 139–197. Available from: Plenum Press: New York.

Gao K-Q, and Shubin NH. 2001. Late Jurassic salamanders from northern China. Nature 410:574-576.

Gorman J, and CL Camp. 1953. A new cave species of salamander of the genus *Hydromantes* from

    California, with notes on habits and habitat. Copeia 1953:39-43.

Graham A. 1999. Late Cretaceous and Cenozoic history of North American vegetation: north of

    Mexico. New York: Oxford University Press, 370 p.

Hammer O and Harper D. 2006. Paleontological data analysis. Oxford: Blackwell. 351 pp.

Hilton WA. 1945. The skeleton of Aneides. J Entomol Zool 37:43-47.

Holman JA 2006. Fossil salamanders of North America. Bloomington: Indiana University Press. 232 p.

Holman JA 1995. Pleistocene amphibians and reptiles in North America. New York: Oxford University

    Press. 254 p.

Jackman TR 1998. Molecular and historical evidence for the introduction of clouded salamanders

    (genus *Aneides*) to Vancouver Island, British Columbia, from California. Can J Zool

    76:1570:1580.

LaDuke TC 1991. Morphometric variability of the precaudal vertebrae of *Thamnophis sirtalis sirtalis* (Serpentes:Colubridae), and implications for interpretation of the fossil record. Unpubl. PhD. Diss., New York: City University of New York.

Lannoo MJ 2005. Amphibian declines: the conservation status of United States species. Berkeley: UC Press. 1094 p.

Larson A and Dimmick WW. 1993. Phylogenetic relationships of the salamander families: An analysis of congruence among morphological and molecular characters. Herpetol Monogr 7:77-93

Larson A, Wake D, and Devitt T. 2003. Caudata. Salamanders. Version 05 September 2006. http://tolweb.org/Caudata/14939/2006.09.05 *in* The Tree of Life Web Project, http://tolweb.org/

Lombard RE and Wake DB. 1986. Tongue evolution in the lungless salamanders, family Plethodontidae. II. Function and evolutionary diversity. J Morph 153:39-79.

Lowe CH. 1950a. Speciation and ecology in salamanders of the genus Aneides. PhD dissertation. Los Angeles: University of California.

Lowe CH 1950b. The systematic status of the salamander *Plethodon hardii*, with a discussion of biogeographical problems in *Aneides*. Copeia 2:92-99.

Maderbacher M, Bauer C, Herler J, Postl L, Makasa L and Sturmbauer C. 2008. Assessment of traditional versus geometric morphometrics for discriminating population of the Tropheus

moorii species complex (Teleostei: Cichlidae), a Lake Tanganyika model for allopatric speciation. J Zool Syst Evol Res 46:153-161.

Mueller RL, Macey JR, Jaekel M, Wake DB, and Boore JL. 2004. Morphological homoplasy, life history evolution, and historical biogeography of plethodontid salamanders inferred from complete mitochondrial genomes. Proc Nat Acad Sci 101:13820-13825.

Petranka JW 1998. Salamanders of the United States and Canada. Washington: Smithsonian Institution Press.

Plotner J, Kohler F, Uzzell F, and Beerli P. 2007. Molecular systematics of amphibians. In: Heatwole H, Tyler M, editors. Amphibian biology, vol. 7: systematics. NSW: Surrey Beatty and Sons. p 2672-2756

Polly PD. and Head JJ. 2004. Maximum-likelihood identification of fossils: taxonomic identification of Quaternary marmots (Rodentia, Mammalia) and identification of vertebral position in the pipesnake *Cylindrophis* (Serpentes, Reptilia). In: Elewa AMT, editor. Morphometrics: Applications in Biology and Paleontology. Berlin: Springer. p. 197-221

Rohlf FJ. tpsDig software. Available at: http://life.bio.sunysb.edu/morph/. Last modified on February 11, 2000.

Thiele K. 1993. The holy grail of the perfect character: the cladistic treatment of morphometric data. Cladistics 9:275-304.

Wake DB, and Jackman TR. 1998. Description of a new species of plethodontid salamander from

    California. Can J Zool 76:1579-1580.

Wake DB 1966. Comparative osteology and evolution of the lungless salamanders, Family

    Plethodontidae. Mem So Cal Acad Sci 4:1-111.

Wake DB 1963. Comparative osteology of the plethodontid salamander genus *Aneides*. J Morph

    113:77-118

Zelditch ML, Swiderski DL, Sheets HD, and Fink WL. 2004. Geometric Morphometrics for Biologists:

    A Primer. San Diego: Elsevier. 433 p.

VITA

LISA NICOLE SCHAAF

Personal data	Place of birth: Erie, Pennsylvania
	Date of birth: September 22, 1983
	Marital status: Single
Education	Mercyhurst Preparatory School, Erie, Pennsylvania, 2002
	B.A. Geoarchaeology, Hamilton College, Clinton, New York, 2006
	M.S. Biology, East Tennessee State University, Johnson City, Tennessee, 2010
Professional Experience	Teaching Assistant, East Tennessee State University, Introduction to Physical Geology, 2008
	Research Assistant, East Tennessee State University, Neogene Vertebrate Paleontology Laboratory, 2007
	Teaching Assistant, Northern Arizona University, Introduction to Environmental Sciences, 2007-2008
	Research Assistant, Northern Arizona University, Laboratory of Quaternary Sciences, 2006